The stochastic pump effect and geometric phases in dissipative and stochastic systems

2009 J. Phys. A: Math. Theor. 42 193001

(http://iopscience.iop.org/1751-8121/42/19/193001)

IOP PUBLISHING JOURNAL OF PHYSICS A: MATHEMATICAL AND THEORETICAL

J. Phys. A: Math. Theor. **42** (2009) 193001 (33pp) doi:10.1088/1751-8113/42/19/193001

TOPICAL REVIEW

The stochastic pump effect and geometric phases in dissipative and stochastic systems

N A Sinitsyn

Center for Nonlinear Studies and Computer, Computational and Statistical Sciences Division, Los Alamos National Laboratory, Los Alamos, NM 87545, USA

Received 8 January 2009, in final form 29 March 2009
Published 22 April 2009
Online at stacks.iop.org/JPhysA/42/193001

Abstract

The success of Berry phases in quantum mechanics stimulated the study of similar phenomena in other areas of physics, including the theory of living cell locomotion and motion of patterns in nonlinear media. More recently, geometric phases have been applied to systems operating in a strongly stochastic environment, such as molecular motors. We discuss such geometric effects in purely classical dissipative stochastic systems and their role in the theory of the stochastic pump effect (SPE).

PACS numbers: 03.65.Vf, 05.10.Gg, 05.40.Ca

(Some figures in this article are in colour only in the electronic version)

1. Introduction

The discovery of the Berry phase [1] revolutionized the study of many quantum-mechanical phenomena. To explain this discovery, consider a quantum system with a Hamiltonian $\hat{H}(\mathbf{k})$, where $\mathbf{k} = \mathbf{k}(t)$ represents a vector of *control parameters* that can change with time along a prescribed path. The state of the quantum system is described by a complex-valued wavefunction Ψ. However, the physical state itself only determines its wavefunction up to a phase because the wavefunctions Ψ and $e^{i\phi}\Psi$ define the same physical state. We assume that, initially, the wavefunction is in one of the nondegenerate eigenstates of the Hamiltonian $\hat{H}(\mathbf{k})$.

If the control parameters $\mathbf{k}$ change with time adiabatically slowly, then the Hamiltonian is explicitly time dependent but the *adiabatic theorem* of quantum mechanics [2] guarantees that the wavefunction will remain an instantaneous eigenstate of the Hamiltonian $\hat{H}(\mathbf{k}(t))$ during the evolution. Assume also that control parameters are changing along a closed contour in the parameter space, so that at the end of the evolution they return to the initial values, as in figure 1. According to the adiabatic theorem, after completing the cycle, the physical state of the system should coincide with the initial one. This theorem does not mean

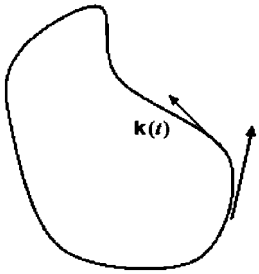

Figure 1. A closed contour in a control parameter space.

that the phase of the wavefunction returns to the initial value. Careful examination shows [1] that the phase picked up after a cyclic evolution can be written as a sum of two components

$$\phi = \phi_{\rm dyn} + \phi_{\rm B}, \tag{1}$$

where the dynamic phase $\phi_{\rm dyn} = -\int_0^T E(t)\,{\rm d}t$ appears even when parameters are fixed, T is the time of cyclic evolution, $E(t)$ is the energy determined as the instantaneous eigenvalue of the Hamiltonian $\hat{H}(\mathbf{k}(t))$, and we assume that $\hbar = 1$. The second contribution in (1) is called the *Berry phase*. It has no stationary counterpart and is purely geometrical, in the sense that it depends only on the choice of the Hamiltonian and on the path in the parameter space. In particular, it does not depend explicitly on time of the evolution T or on the rate of motion along the contour. Given the dependence of the eigenstate $|u\rangle$ of the Hamiltonian on $\mathbf{k}$ in some gauge, the Berry phase is given by

$$\phi_{\rm B} = \oint_{\mathbf{c}} \mathbf{A}\cdot\mathbf{k}, \qquad \mathbf{A} = \langle u|{\rm i}\partial_{\mathbf{k}}u\rangle, \tag{2}$$

where $\mathbf{c}$ is the contour in the space of control parameters, and $\mathbf{A}$ is called *the Berry connection* (see Griffiths [3] for a pedagogical derivation). The cyclic Berry phase is gauge invariant and has measurable effects, which have been confirmed experimentally.

Berry's discovery has a rich prehistory. As Berry himself pointed out [4], a number of effects in quantum mechanics had been related to the unusual phase evolution of the wavefunction even before Berry's discovery [1]. Other historical antecedents can be found, for example, in the first efforts to create a semiclassical theory of the anomalous Hall effect [5, 6]. However, it was Berry's work that unified all these known geometric effects under a universal theoretical framework. This framework has proved very useful in uncovering new effects and has provided the theoretical groundwork for entire branches of physics such as topological quantum computations [11], the quantum theory of polarization [10] and the theories behind various extraordinary Hall effects [7–9].

The Berry phase is an example of the *anholonomy* effect encountered in the theory of differential equations. Anholonomy can be non-rigorously defined as failure of vectors return to their initial values after a parallel transport along a closed contour.

Since there are both quantum-mechanical and classical-mechanical antecedents of the geometric phase, it is natural to ask whether there are also antecedents in stochastic processes. Here, we should point out that there is a fundamental difference from quantum mechanics, which prevents direct analogies. While the state of a quantum system defines the wavefunction only up to an overall phase, a classical ergodic stochastic system can be described by a probability vector, without allowing any additional freedom in its definition. For example, consider a *Markov process*, i.e. a stochastic process whose future evolution depends only on the

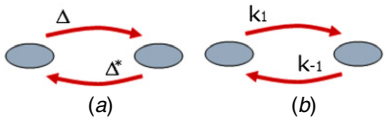

Figure 2. Two-state systems: (a) quantum and (b) stochastic.

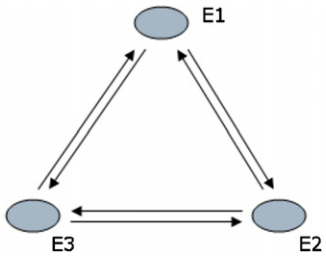

Figure 3. A three-state Markov chain. This model can be considered as a minimal model to describe the stochastic behavior of a molecular motor in figure 12.

present state but does not depend on the past. The evolution of the probability vector satisfies equations which are reminiscent of the quantum-mechanical evolution. Figure 2 shows the simple example of a two-state quantum system and its stochastic counterpart. In both cases the evolution is described by linear differential equations with 2×2 evolution matrices. In the quantum-mechanical case, the amplitudes u_1 and u_2 of two states evolve according to the Schrödinger equation

$$\mathrm{i}\frac{\mathrm{d}}{\mathrm{d}t}\begin{pmatrix} u_1 \\ u_2 \end{pmatrix} = \begin{pmatrix} \epsilon_1(t) & \Delta(t) \\ \Delta^*(t) & \epsilon_2(t) \end{pmatrix}\begin{pmatrix} u_1 \\ u_2 \end{pmatrix}, \tag{3}$$

while the continuous two-state Markov process, with probabilities p_1 and p_2 of the first and the second states, is defined by the differential system [12]

$$\frac{\mathrm{d}}{\mathrm{d}t}\begin{pmatrix} p_1 \\ p_2 \end{pmatrix} = \begin{pmatrix} -k_1(t) & k_{-1}(t) \\ k_1(t) & -k_{-1}(t) \end{pmatrix}\begin{pmatrix} p_1 \\ p_2 \end{pmatrix}, \tag{4}$$

where parameters k_1 and k_{-1} are called *kinetic rates*. They describe how often a system jumps from one state into the other. In spite of the similarity of equations (3) and (4), it is well known that a quantum-mechanical, cyclically driven two-state system can have a nontrivial geometric Berry phase, but that is not true for its stochastic counterpart. For given values of parameters, an ergodic Markov chain has a unique steady state. Under slow evolution of parameters, the probability vector will simply follow the path of instantaneous steady-state values, returning to the initial vector after the parameters complete a full cycle.

This example shows that, in an obvious sense, the Markov process does not lead to adiabatic geometric phases. However, this conclusion is restricted only to the evolution of the probability vector for a present state. There are other characteristics describing stochastic processes. For example, one can consider stochastic transitions among three states in figure 3 and ask what is the probability that the system makes exactly n full cycles in a clockwise direction by the given time t. In the following sections, we will derive the evolution equations for similar quantities and show that geometric phases do play an important role in their evolution.

Anholonomies also play a central role in classical thermodynamics. The Carnot cycle is an example of a thermodynamic process exhibiting anholonomy [13]. Statistical properties of

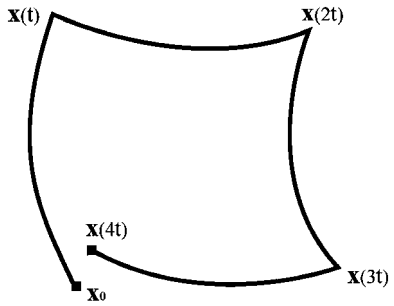

Figure 4. Trajectory of $\mathbf{x}$ in response to a periodic infinitesimal path in the space of control parameters $\{u_i\}$.

a system in thermodynamic equilibrium can be specified by a set of parameters, such as the volume, the pressure and the temperature. Slow cyclic changes of these parameters merely produce cyclic changes of the equilibrium properties, so, as in the example of a two-state Markov chain, a driven system returns to the initial state in a statistical sense by the end of a cycle. However, if one looks at the same process from a more general point of view, namely including effects of this process not only on the given system, but also on systems in contact with it, a cyclic adiabatic evolution of control parameters usually does not lead to the same finite state in the full phase space. The laws of thermodynamics predict that the system converts part of the absorbed energy into production of the work. Moreover, for adiabatically slow evolution, the work produced depends only on the choice of the contour in the parameter space, but depends neither on the rate of motion nor on the mechanism of coupling to the environment. This means that the work can be expressed as a contour integral over the path in the space of control parameters. For example, for a gas in a reservoir with variable volume V and temperature T, the work W produced per cycle is

$$W = \oint_{\mathbf{c}(T,V)} p(T, V) \cdot \mathrm{d}V, \tag{5}$$

where $p(T, V)$ is the pressure.

The property of dynamic systems to change their state in response to a periodic perturbation with zero bias has been widely used in control theory [14]. Look e.g. at the simple input/output model described by differential equations

$$\dot{x}^i = f^i_j(\mathbf{x}) u_j(t), \tag{6}$$

where f_j are smooth functions of $\mathbf{x}$ and $u_j(t)$ represent control parameters. One can consider a simple periodic evolution in the control parameter space by setting $u_i = \delta_{i,1}$ during an infinitesimal time interval t, where $\delta_{i,j}$ is 1 when $i = j$ and 0 otherwise. After this, one sets $u_i = \delta_{i,2}$ during the following time interval $(t, 2t)$, then takes $u_i = -\delta_{i,1}$ for $(2t, 3t)$, and finishes with $u_i = -\delta_{i,2}$ during $(3t, 4t)$.

An easy perturbative calculation shows that, after one such an infinitesimal evolution in the space of control parameters with zero bias, the vector $\mathbf{x}$ does not generally return to the initial state but rather acquires an additional correction, as in figure 4, such that

$$\mathbf{x}(4t) = \mathbf{x}_0 + t^2[\mathbf{f}_1, \mathbf{f}_2](\mathbf{x}_0) + \mathrm{O}(t^3), \tag{7}$$

where the operation $[\mathbf{f}_1, \mathbf{f}_2]^i = \left(f_1^j \partial f_2^i / \partial x^j\right) - \left(f_2^j \partial f_1^i / \partial x^j\right)$ is called the *Lie brackets* of the vector fields $\mathbf{f}_1$ and $\mathbf{f}_2$. In general, the value at $\mathbf{x}_0$ of the Lie bracket $[\mathbf{f}_1, \mathbf{f}_2]$ can even be linearly independent of $\mathbf{f}_1(\mathbf{x}_0)$ and $\mathbf{f}_2(\mathbf{x}_0)$. This phenomenon is exploited in Chow's theorem

which, together with the theorem of Frobenius, describes the space of configurations that can be reached using only a prescribed set of vector fields to get around [15].

Although the history of anholonomy effects reaches at least as far back as the 19th century, a complete survey of its development is beyond the scope of this review and we will not pursue it further. Instead, we will concentrate on applications of geometric phases to stochastic and dissipative processes. These topics have attracted attention relatively recently due, in part, to the success of the Berry phase in quantum mechanics. We attempted to make the review accessible to an audience not familiar with the mathematical theory of fiber bundles. This review is also not about the large body of work related to decoherence effects on quantum-mechanical Berry phases or on geometric phases in chaotic non-dissipative systems. The reader should consult [2, 16–19] for an introduction to these topics.

The structure of this review is as follows. Section 2 reviews extensions of the Berry phase idea to non-unitary evolution. Section 3 describes the theory and applications of geometric phases in dissipative systems with a continuous symmetry of steady-state solutions. One important application is to control of pattern motion in nonlinear media. Section 4 briefly reviews the geometric theory of locomotion of micro-organisms. In section 5, we introduce the stochastic pump effect and its relation to geometric phases in the evolution of the moment generating functions. In section 6, we generalize the concept of the geometric phase in stochastic processes to noncyclic evolutions. In section 7, we explain how geometric phases can influence the kinetics of slow variables in a coarse-grained description of a stochastic process with a hierarchy of important timescales. This is regarded as a stochastic analogue of the quantum-mechanical Born–Oppenheimer approximation. We also study stochastic analogues of Berry phases from this point of view. The reader who is not interested in complicated mathematical details might prefer to skip section 7 on a first reading. In section 8, we review the geometric phases in the 'limit cycle' evolution. Section 9 is about constraints that detailed balance conditions impose on geometric effects in systems near thermodynamic equilibrium. In section 10, we apply some of the techniques we have discussed to the theory of molecular motor operations. In section 11, we outline several directions for possible future research.

2. Geometric phases in non-unitary evolution

Non-unitary evolution is often considered in quantum-mechanical problems, where the coupling to the environment is described phenomenologically by introducing extra parameters in the equations of motion for a density matrix or a wavefunction. In many physical problems one can encounter evolution equations, similar to quantum-mechanical ones but with a non-Hermitian operator replacing the Hamiltonian. Examples can be found in electronic circuits [20], optics [21] and acoustics [22]. The evolution of any dissipative system near a stable point or a limit cycle can be linearized and assume a form similar to the quantum-mechanical Schrödinger equation for a state vector. Motivated by the success of the quantum-mechanical Berry phase, several studies [23–26] were devoted to geometric phases in systems with non-Hermitian Hamiltonians. The models considered could generally be written in the form

$$\frac{\mathrm{d}}{\mathrm{d}t}|u\rangle = \hat{H}(\mathbf{k})|u\rangle, \tag{8}$$

where $\hat{H}$ is an arbitrary $N \times N$ matrix and $|u\rangle$ is an N-vector.

Imitating the derivation of the quantum-mechanical Berry phase in the adiabatic limit leads one to a similar result: if the vector $|u\rangle$ at the initial moment of the evolution is one of

the eigenstates of the matrix $\hat{H}(\mathbf{k})$, i.e. if

$$\hat{H}|u(0)\rangle = \varepsilon|u(0)\rangle, \tag{9}$$

then after a slow cyclic evolution of parameters, the vector $|u\rangle$ generally returns to the initial one up to a factor

$$|u(T)\rangle = \mathrm{e}^{-\oint_{\mathbf{c}} \mathbf{A}\cdot\mathrm{d}\mathbf{k}}\, \mathrm{e}^{\int_0^T \mathrm{d}t\varepsilon(t)}|u(0)\rangle, \tag{10}$$

which can be separated into dynamic and geometric parts. Strictly speaking, the values in the exponents in (10) are not phases because they are no longer purely imaginary. However, it is generally accepted to use the term, 'phase', because of the strong analogy with quantum-mechanical phases. Berry [25] pointed that it is convenient to express the geometric phase by introducing also the left eigenstates of the Hamiltonian $\hat{H}(\mathbf{k})$, such that

$$\langle u|\hat{H} = \langle u|\varepsilon. \tag{11}$$

The eigenvalues for left and right eigenvectors coincide. For a non-Hermitian Hamiltonian, the eigenvalues are no longer real and the components of the left eigenvector are no longer complex conjugates of the right eigenvector. In other respects, there is a strong similarity with quantum-mechanical Berry phases, e.g. the connection $\mathbf{A}$ can be written as

$$\mathbf{A} = \frac{\langle u|\partial_{\mathbf{k}} u\rangle}{\langle u|u\rangle}. \tag{12}$$

Non-unitary evolution does not necessarily describes a dissipation. The geometric phases with a non-Hermitian Hamiltonian that realizes transformations of the group $SU(1,1)$ (i.e. transformations that preserve the form $|z_1|^2 - |z_2^2|$ of a complex-valued 2-vector (z_1, z_2)), have attracted considerable attention because of their applications to squeezed states [27–30], and a number of models in classical mechanics and optics [31–33]. The group $SU(1,1)$ is a covering group of the 3D Lorentz group. The corresponding geometric phase is responsible for a variety of relativistic effects, such as Thomas precession [34, 35]. We refer the interested reader to the review [36]. More important for our subject is that the group $SU(1,1)$ is isomorphic to the group $SL(2, R)$ of 2×2 matrices with real entries and the unit determinant. The $SL(2, R)$ evolution can be used to describe a classical dissipative system. Corresponding geometric phases were studied both theoretically and experimentally in connection with light propagation through a set of polarizers [37–39]. Recently, the relation of this geometric phase to the stochastic pump effect was discussed in [40].

The geometric phase in equation (10) was generalized to non-Abelian and non-adiabatic evolutions [26, 41] and a number of applications were proposed, e.g. to optically active refracting media [25]. One interesting property of non-Hermitian Hamiltonians, not found in quantum mechanics, is the possibility of so-called exceptional points in the spectrum. If a contour encloses such points, the eigenvalues of the Hamiltonian are not single valued along this contour. A simple example is the following 2×2 matrix, which depends on a complex parameter z and which has 0 as an exceptional point:

$$\begin{pmatrix} 0 & 1 \\ z & 0 \end{pmatrix}, \qquad z \in \mathbb{C} - \{0\}.$$

Its eigenvalues $\lambda_\pm = \pm\sqrt{z}$ are double-valued functions on the space $\mathbb{R}^2 - \{0\}$. Encircling such points, the eigenvectors acquire a geometric phase of a new type which has been studied theoretically in [42–45] and observed in experiments [46, 47].

In spite of this progress, one might think that the geometric phase in dissipative evolution would be insignificant in comparison with the dynamic part in (10) on the grounds that the latter becomes either exponentially large or exponentially small with time. However, not all

modes in dissipative evolution grow or decay exponentially since the matrix $\hat{H}$ might also have zero modes, i.e. one or several linearly independent states with a zero eigenvalue. If all other modes decay quickly, according to (10), the evolution of such a dissipative system in the adiabatic limit should instead be governed by the geometric phases. More generally, geometric phases can also be important when, for fixed values of parameters, a system relaxes to a limit cycle. In that case, the corresponding eigenvalue is purely imaginary.

3. Control over pattern position and orientation

In early 1990s, Landsberg [48, 49], and independently Ning and Haken [50, 51], suggested that geometric phases should generally appear in many classical systems which can be described by a set of nonlinear differential equations with a one-parameter group of symmetry transformations. In such a system, it is possible to reduce the evolution equations to a form in which one of the variables does not affect the evolution of the others, that is

$$\frac{\mathrm{d}\mathbf{Y}}{\mathrm{d}t} = \mathbf{F}(\mathbf{Y}, \boldsymbol{\lambda}), \qquad \frac{\mathrm{d}\Theta}{\mathrm{d}t} = H(\mathbf{Y}), \tag{13}$$

where Θ and the vector $\mathbf{Y}$ represent generalized coordinates of the system while $\mathbf{F}$ and H are nonlinear functions of the coordinate vector $\mathbf{Y}$, but not of Θ. Assume that the system is initially at the steady state and that the parameter vector $\boldsymbol{\lambda}$ changes slowly with time. Landsberg considered the case when the evolution of the variable $\mathbf{Y}$ is dissipative, so that if parameters $\boldsymbol{\lambda}$ are time independent, $\mathbf{Y}$ relaxes to a steady-state value $\mathbf{Y}^*(\boldsymbol{\lambda})$. In that case, for adiabatically slow evolution of $\boldsymbol{\lambda}$, $\mathbf{Y}$ simply follows a quasi-steady-state trajectory up to a small non-adiabatic correction

$$\mathbf{Y}(t) \approx \mathbf{Y}^* + D\mathbf{F}^{-1}(\mathbf{Y}^*)\partial_t \mathbf{Y}^*, \tag{14}$$

where $D\mathbf{F} = (\partial\mathbf{F}/\partial\mathbf{Y})_{\mathbf{Y}=\mathbf{Y}^*}$ is the linearization of the vector function $\mathbf{F}$, and $D\mathbf{F}^{-1}$ is the inverse of the linear function $D\mathbf{F}$. However, one should not assume that Θ can be uniquely determined by given values of the control parameters. Due to the symmetry $\Theta \to \Theta + \delta\theta$ of equation (13), where $\delta\theta$ is an arbitrary constant, the steady-state value of Θ is not specified. Hence Θ does not have to return to its initial value after the parameters $\boldsymbol{\lambda}$ complete a full cycle. Landsberg showed in [49] that, after a cyclic evolution, the variable Θ changes by an amount given by a trivial dynamic part $\Delta\Theta_{\mathrm{dyn}} = \int \mathrm{d}t\, H(\mathbf{Y}^*(t))$ plus a geometric contribution

$$\Delta\Theta_{\mathrm{geom}} = \oint_{\mathbf{c}} \mathbf{A}\cdot\mathrm{d}\boldsymbol{\lambda}, \qquad \mathbf{A} = DH(\mathbf{Y}^*)D\mathbf{F}^{-1}(\mathbf{Y}^*)\partial_{\boldsymbol{\lambda}}\mathbf{Y}^*, \tag{15}$$

where $DH = \partial H/\partial\mathbf{Y}|_{\mathbf{Y}=\mathbf{Y}^*}$ is the linearization of the function H near the point $\mathbf{Y}^*$.

Suppose, that instead of a vector $\mathbf{Y}$ with discrete set of entries, we deal with continuous systems. The vector index then becomes a continuous coordinate and $\mathbf{Y}$ is a function of this coordinate. To generalize (15) to such continuous systems, Landsberg considered equations of the form

$$\frac{\mathrm{d}\Psi(t,x)}{\mathrm{d}t} = \hat{F}(x, \boldsymbol{\lambda})\Psi(t,x), \tag{16}$$

where $\hat{F}$ is now a nonlinear operator, which depends on time only through time-dependent control parameters $\boldsymbol{\lambda}$, and where the evolution equation (16) is assumed to be invariant under a continuous group G of symmetries, such as the group of translations in the direction of the coordinate x.

Let $|\psi(x)\rangle$ be a *stationary pattern profile*, i.e. a time-independent solution to (16) for constant $\boldsymbol{\lambda}$. Let $D\hat{F}$ be the differential operator, which is the linearization of the operator $\hat{F}$ near the solution $|\psi(x)\rangle$, and let $\langle v_0|$ be the zero mode of the differential operator $D\hat{F}^+$,

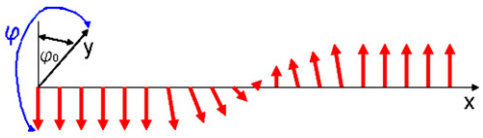

Figure 5. The wire with a hard anisotropy axis along it and a domain wall between two opposing magnetization directions. Easy axis anisotropy is perpendicular to the x-direction, and makes an angle φ_0 with a y-axis. Red vectors show the direction of the local magnetization.

which is the *conjugated differential operator* to $D\hat{F}$, in the sense that $\int g(Df) = \int (D^+ g) f$. Landsberg showed that after a cyclic evolution in the parameter space, the stationary pattern will change by a geometric shift $\Delta\Theta_{\text{geom}}$, given by

$$\Delta\Theta_{\text{geom}} = \oint_{\mathbf{c}} \mathbf{A} \cdot d\boldsymbol{\lambda}, \qquad \mathbf{A} = -\frac{\langle v_0 | \partial_{\boldsymbol{\lambda}} \psi \rangle}{\langle v_0 | \hat{\chi} \psi \rangle}, \tag{17}$$

along the symmetry direction, where $\hat{\chi}$ is the generator of transformations of the symmetry group G.

Equation (17) can be illustrated by a following simple example [52, 53]. Consider a 1D ferromagnetic wire with a strong hard axis along it, which favors a magnetization direction transverse to the wire, as shown in figure 5. Assume that a fixed set of rectangular coordinate axes has been chosen, with the x-axis along the wire. We also assume the presence of a weak transverse anisotropy, so that the magnetization energy is described by the energy functional

$$E \approx \int \mathrm{d}x \{ J(\partial\varphi/\partial x)^2 + K \sin^2(\varphi - \varphi_0) \}, \tag{18}$$

where φ is the magnetization angle with the y-axis, and the parameter φ_0 is the angle that the transverse anisotropy axis makes with the y-axis (figure 5).

In the limit of strong dissipation, the evolution of the variable $\varphi(x, t)$ is given by

$$\alpha \partial_t \varphi = -\frac{\delta E}{\delta \varphi} = 2J\partial_x^2 \varphi - K \sin[2(\varphi - \varphi_0)], \tag{19}$$

where α is a damping constant. Note that equation (19) is invariant under the translation $x \to x - \delta x$, which justifies the use of the geometric theory of [48]. The generator of this symmetry is $\hat{\chi} = -\partial_x$.

At equilibrium, the ground state of (18) is doubly degenerate at $\varphi = \varphi_0$ and $\varphi = \varphi_0 + \pi$. Consider the stationary solution of (19) describing a *domain wall* connecting these two states

$$\varphi^{\text{dw}}(x; \varphi_0, x_0) = \varphi_0 + 2\tan^{-1} \mathrm{e}^{(x - x_0)/\Delta}, \qquad \Delta = \sqrt{J/K_0}, \tag{20}$$

where x_0 and Δ can be called respectively the *position* and the *size* of the domain wall. Assume that the parameter φ_0 is slowly time dependent and varies from 0 to 2π as the transverse anisotropy axis performs one rotation around the x-direction. One can realize this situation, for example, by physically rotating a wire. In our model, φ_0 is the control parameter, and equation (17) gives

$$\delta x_0 = \oint \frac{\int_{-\infty}^{\infty} \mathrm{d}x [v_0(x) \partial_{\varphi_0} \varphi^{\text{dw}}(x)]}{\int_{-\infty}^{\infty} \mathrm{d}x [v_0(x) \partial_x \varphi^{\text{dw}}(x)]} \, \mathrm{d}\varphi_0, \tag{21}$$

where $v_0(x)$, given by

$$v_0(x) = \frac{\Delta}{\cosh((x - x_0)/\Delta)}, \tag{22}$$

is the zero mode of the self-adjoint operator

$$D\hat{F} = D\hat{F}^{+} = 2J\partial_x^2 - 2K\cos[2(\varphi^{\mathrm{dw}}(x;\varphi_0,x_0) - \varphi_0)]. \tag{23}$$

Substituting this value of $v_0(x)$ into (21) we find

$$\delta x_0 = \int_0^{2\pi} A_{\varphi_0}\mathrm{d}\varphi_0, \qquad A_{\varphi_0} = \pi\Delta/2, \tag{24}$$

which was derived in [53] using the secular perturbation theory.

A number of theoretical and experimental studies of the motion of domain walls in liquid crystals under the influence of periodic perturbations have been performed [52, 54–57], but the role of the geometric phase has not been discussed. Landsberg's theory was aimed at control of wave patterns in nonlinear media. Such control was discussed in more detail for specific applications to nonlinear chemical reactions [58], nonlinear optics [59], hydrodynamics [60] and semiconductor microresonators [61]. Optical applications proposed by Ning and Haken were extended by Toronov and Derbov [62, 63].

Studies of special problems with a mathematical structure similar to the Landsberg–Ning–Haken formalism can be found even prior to [48, 49]. For example, the use of a rotating electric field was suggested as a means of separating chiral molecules in solution [64, 65]. Recently this idea was extended to the gaseous state, but the proposed effect is expected to be observed in the non-adiabatic regime [66]. Geometric phases can also contribute to the anomalous shift of the trajectory of a magnetic bubble in a rotating nonuniform magnetic field, which is called the *skew-deflection effect* [67].

Control over the motion of domain walls and other topological defects has been extensively studied in magnetic materials [67–70]. The example of the domain wall shown above demonstrates that the projection of dynamics on the collective degrees of freedom should be performed with extra care to account for possible geometric phase effects. For example, in the micromagnetics literature, one often finds that the equations of motion for the collective coordinates $\boldsymbol{\xi}$ read [69]

$$-\partial U/\partial\boldsymbol{\xi} - \Gamma\dot{\boldsymbol{\xi}} + G\dot{\boldsymbol{\xi}} = 0, \tag{25}$$

where $-\partial U/\partial\boldsymbol{\xi}$ is the generalized force, Γ is the symmetric dissipation matrix and G is the antisymmetric gyrotropic matrix. However, equation (25) can lead to problems. In the case of a domain wall (20), one can attempt to work with a single collective coordinate representing the position of the domain wall, and to regard the angle φ and the size of the domain wall Δ as fast variables. This choice might seem natural in view of the fact that translation is the only continuous symmetry in the model and should dominate the physics at low energies and under slow perturbations. However, in the model under consideration, the wall was moving because some parameters became time dependent. In the static case, there are no forces on the chosen collective degrees of freedom. Thus equation (25) can acquire extra geometric terms in explicitly time-dependent situations, and is therefore not, in itself, sufficiently general even when only slow changes of parameters are considered. As another word of caution, we note that the translational symmetries in real applications are only approximate for standard magnetic materials because of the presence of impurities and discreteness of the lattice. As discussed in [53], this is a serious obstacle to purely geometric control over magnetic defects in practical applications.

4. Self-propulsion at low Reynolds numbers

One of the first applications of geometric phases in dissipative systems was proposed by Shapere and Wilczek [71, 72] in their description of locomotion of microscopic organisms in a

viscous fluid. This theory was based on the well-known observation that the motion of living organisms at low Reynolds numbers is, in fact, geometrical. Microscopic living organisms propel themselves in a liquid by performing periodic changes of their shapes. These changes correspond to noncyclic motion in a larger space, whose points describe the shape of the body, its position and its overall orientation. One can choose a *gauge* in this phase space, i.e. a rule to determine the position and the orientation of the body of any given shape with respect to a fixed coordinate system in the three-dimensional space. Using such a gauge one can characterize the state of the body by a set of coordinates (x, α), where α is a vector of shape parameters and $x = (\mathbf{r}, \phi)$ consists of the position $\mathbf{r}$ and orientation ϕ of the body.

Body shapes are assumed to be directly controllable by the organism subject to certain constraints such as conservation of volume, which allow only finite and quasi-periodic changes of $\boldsymbol{\alpha}$. The body interacts with a high viscosity liquid which is described by the incompressible Navier–Stokes equation. This equation should be solved with no-slip boundary conditions at the surface of the organism to guarantee the absence of force and a torque on it. For slow changes of shape, these no-slip conditions are expressible in terms of the first partial derivatives of x with respect to time. In particular, they are automatically satisfied by non-moving bodies. After eliminating the degrees of freedom of the liquid by solving the Navier–Stokes equation, the equation that connects changes of x and $\boldsymbol{\alpha}$ follows from the boundary conditions and has the form

$$\mathrm{d}x = \mathbf{A}(\boldsymbol{\alpha}) \cdot \mathrm{d}\boldsymbol{\alpha}, \tag{26}$$

where the connection $\mathbf{A}$ is defined on the space of body shapes. Integration over a closed path $\mathbf{c}$ in the space of body shapes leads to the purely geometric result that $\delta x = \oint_{\mathbf{c}} \mathbf{A}(\boldsymbol{\alpha}) \cdot \mathrm{d}\boldsymbol{\alpha}$.

The geometric theory of locomotion at low Reynolds numbers has found too many applications to summarize here. Fortunately, fairly good introductions and reviews are already available [73–75]. Here we only mention that the theory was applied to determine optimal protocols for cell body changes [76–80]. It was found that such optimal moves are similar to those observed in some organisms [76, 79]. Discussions of simple illustrative models can be found in [77, 81]. An application of the theory for the propulsion of microscopic objects by manmade motors at low Reynolds numbers can be found in [82].

5. Stochastic pump

A *stochastic pump* is a stochastic system that responds with nonzero on average currents to periodic perturbations [83–87]. We will call such currents the *pump currents*. A stochastic pump resembles a *quantum pump* [88–93]. In the latter, nonzero currents appear under similar circumstances but originate from purely quantum-mechanical effects. The stochastic pump effect (SPE) was observed in frequency-locked electronic turnstile devices [94, 95] and in enzymatic reactions [96]. Recently, it was studied experimentally in transport through a conical nanopore, where strong pump current variations were found as a function of the relative phase of applied voltage signals [97].

One of the simplest models of the SPE is illustrated in figure 6. In this model, the central bin system **B** can have at most one particle inside. The bin is connected to the *absorbing state* **S** from the left and the absorbing state **R** from the right. The term absorbing state means here that any number of particles can enter this state or leave it. Kinetic rates in the model are shown in figure 6. If the bin is empty, then, with rates k_1 or k_{-2}, a particle jumps into the bin either from the left or from the right, respectively. If the bin contains a particle, transitions into the bin are forbidden until this particle escapes to the left or to the right, which it does, respectively, with rates k_{-1} and k_2. We assume that the kinetic rates are time dependent, i.e.

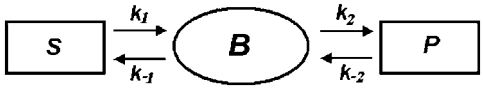

Figure 6. A simple system demonstrating the stochastic pump effect.

they are control parameters, and we are interested in currents of particles from one absorbing state into the other one. The SPE in this model has been studied in great detail [98–102]. Even so, due to the simplicity of the kinetic scheme in figure 6, the average current can be studied analytically along with its fluctuations [100].

The model in figure 6 can be used to describe charge transport through a quantum dot in the Coulomb blockade regime [103], where absorbing states represent conducting leads, and the bin represents the quantum dot with at most one electron inside. It also serves as a model of molecular fluxes through an ion channel connecting two compartments in a living cell [96, 152].

In what follows, we will consider the realization of the model in figure 6 in the enzymatic mechanism of Michaelis–Menten type [104], which is defined as the following chemical reaction:

$$E + S \underset{k_{-1}}{\overset{k_1}{\rightleftarrows}} ES \underset{k_{-2}}{\overset{k_2}{\rightleftarrows}} E + P, \tag{27}$$

where S and P are called *substrate* and *product*, and E is an *enzyme* molecule. Here, we assume a situation with a formally infinite number (a *sea*) of substrate and product molecules but with only a single enzyme molecule. Either S or P can combine with the enzyme E to produce an unstable complex which we will refer to as the *bound* state of enzyme. This complex can then dissociate into either E and S or into E and P. These dissociated states will be referred to as the *free* states. Here it is important to note that, even if ES is formed from E and P (resp. E and S), it can freely dissociate into either E and P or into E and S. In terms of the model of figure 6, the free states are those in which the bin is empty, while the bound state is that in which the bin is filled. The sea of substrate molecules is represented by the **S**-state and the sea of product molecules is represented by the **P**-state in figure 6.

We define *the moment generating function* for the number of transitions, n, in time T from ES (the bin with a particle) into $E + P$ (the absorbing state **P**) by

$$Z(\chi, T) \equiv \mathrm{e}^{S(\chi,T)} = \sum_{n=-\infty}^{+\infty} P_n(T)\, \mathrm{e}^{\mathrm{i}n\chi}, \tag{28}$$

where P_n is the probability of the event that, by time T, there will be n new product molecules created, counting the opposite process with a minus sign. $S(\chi, T)$ is the *cumulant generating function* of the number of transitions, because it determines all cumulants of the particle flux. For example, the mean $\langle n(T)\rangle$ and the variance $\mathrm{var}(n(T))$ are given, respectively, by

$$\langle n(T)\rangle = (-\mathrm{i})\, \frac{\partial S(\chi, T)}{\partial \chi}\bigg|_{\chi=0}, \qquad \mathrm{var}(n(T)) = (-\mathrm{i})^2\, \frac{\partial^2 S(\chi, T)}{\partial \chi^2}\bigg|_{\chi=0}. \tag{29}$$

In order to derive the evolution equation for the generating function (28), it is convenient to introduce the generating functions $U_E = \sum_{n=-\infty}^{\infty} P_{nE}\, \mathrm{e}^{\mathrm{i}n\chi}$ and $U_{SE} = \sum_{n=-\infty}^{\infty} P_{nSE}\, \mathrm{e}^{\mathrm{i}n\chi}$, where P_{nE} and P_{nSE} are the following probabilities: P_{nE} is the probability that, at a given time, the system is in a free state and the number of product molecules created is n, and P_{nSE} is the probability that enzyme is in a bound state and the number of product molecules created

is also n [166]. The master equations for P_{nE} and P_{nSE} are then

$$\begin{aligned}\frac{\mathrm{d}}{\mathrm{d}t}P_{nE} &= -(k_1+k_{-2})P_{nE} + k_{-1}P_{nSE} + k_2 P_{(n-1)SE},\\ \frac{\mathrm{d}}{\mathrm{d}t}P_{nSE} &= -(k_{-1}+k_2)P_{nSE} + k_1 P_{nE} + k_{-2}P_{(n+1)E}.\end{aligned} \tag{30}$$

Multiplying (30) by $\mathrm{e}^{\mathrm{i}\chi n}$ and summing over n we find

$$\frac{\mathrm{d}}{\mathrm{d}t}\begin{pmatrix}U_E\\ U_{SE}\end{pmatrix} = \hat{H}(\chi,t)\begin{pmatrix}U_E\\ U_{SE}\end{pmatrix}, \tag{31}$$

where

$$\hat{H}(\chi,t) = \begin{pmatrix}-k_1-k_{-2} & k_{-1}+k_2\,\mathrm{e}^{\mathrm{i}\chi}\\ k_1+k_{-2}\,\mathrm{e}^{-\mathrm{i}\chi} & -k_{-1}-k_2\end{pmatrix}. \tag{32}$$

If we set $n = 0$ at an initial moment $t = 0$, then the initial conditions for (31) are $U_E(t=0) = p_E(0)$, and $U_{SE}(t=0) = p_{SE}(0)$, where $p_E(0)$ and $p_{SE}(0)$ are probabilities that the enzyme is respectively free or in the substrate–enzyme complex. Also, note that $Z(\chi,t) = U_E(\chi,t) + U_{SE}(\chi,t)$. Thus, formally, the moment generating function in (28) can be expressed as the following average of the evolution operator:

$$Z(\chi,t) = \langle 1|\hat{T}\big(\mathrm{e}^{\int_0^t \hat{H}(\chi,t)\,\mathrm{d}t}\big)|p(0)\rangle, \tag{33}$$

where $\langle 1| = (1,1)$, where $|p(0)\rangle = (p_E(0), p_{SE}(0))$ is the vector of initial probabilities of enzyme states and where $\hat{T}$ is the time-ordering operator.

A derivation of the adiabatic approximation for (33) can be found in [100] but the general discussion of section 2 shows that the generating function for a slow cyclic evolution of parameters is an exponential of the sum of two terms: one geometric and one dynamic,

$$Z(\chi) = \mathrm{e}^{S_{\mathrm{geom}}(\chi)+S_{\mathrm{dyn}}(\chi)}. \tag{34}$$

Let $\varepsilon_0(\chi)$ be the instantaneous eigenvalue of $\hat{H}(\chi,t)$ with the larger real part, let $\kappa_\pm = k_{\pm1}k_{\pm2}$, let $e_{\pm\chi} = \mathrm{e}^{\pm\mathrm{i}\chi} - 1$ and let $K = \sum_m k_m$ where $m = -2, -1, 1, 2$. Then the *dynamic part* is given by

$$S_{\mathrm{dyn}}(\chi) = \int_0^T \mathrm{d}t\;\varepsilon_0(\chi,t) = -\frac{1}{2}\int_0^T \mathrm{d}t\big[K - \sqrt{K^2 + 4(\kappa_+ e_\chi + \kappa_- e_{-\chi})}\big], \tag{35}$$

The problem of degeneracy of eigenvalues cannot appear here because the eigenvalue $\varepsilon_0(\chi,t)$ corresponds to the unique steady state of the system. Here, we note that the vector of kinetic rates $\mathbf{k}$ depends on t and describes a contour $\mathbf{c}$ in the parameter space. Next, denoting by $|u_0(\chi,\mathbf{k})\rangle$ the eigenvector corresponding to $\varepsilon_0(\chi,\mathbf{k})$, the *geometric part* $S_{\mathrm{geom}}(\chi)$ is given by equation

$$S_{\mathrm{geom}}(\chi) = -\oint_{\mathbf{c}} \mathbf{A}\cdot\mathrm{d}\mathbf{k}, \qquad A_m = \langle u_0(\chi,\mathbf{k})|\partial_{k_m}|u_0(\chi,\mathbf{k})\rangle. \tag{36}$$

There is an obvious analogy between the geometric part of the cumulant generating function (36) and the Berry phase in quantum mechanics (2). The geometric phase $S_{\mathrm{geom}}(\chi)$ in (34) was discovered by Sinitsyn and Nemenman in [100].

If parameters k_1 and k_{-2} are time dependent, while k_2 and k_{-1} are constants, then

$$\oint_{\mathbf{c}} \mathbf{A}\cdot\mathrm{d}\mathbf{k} = \iint_{\mathbf{s_c}} \mathrm{d}k_1\,\mathrm{d}k_{-2}F_{k_1,k_{-2}}, \tag{37}$$

where $\mathbf{s_c}$ is a surface whose boundary is the contour $\mathbf{c}$, and

$$F_{k_1,k_{-2}} = \left\langle\frac{\partial u_0}{\partial k_1}\middle|\frac{\partial u_0}{\partial k_{-2}}\right\rangle - \left\langle\frac{\partial u_0}{\partial k_{-2}}\middle|\frac{\partial u_0}{\partial k_1}\right\rangle. \tag{38}$$

$F_{k_1,k_{-2}}$ is the analogue of the quantum-mechanical *Berry curvature*.

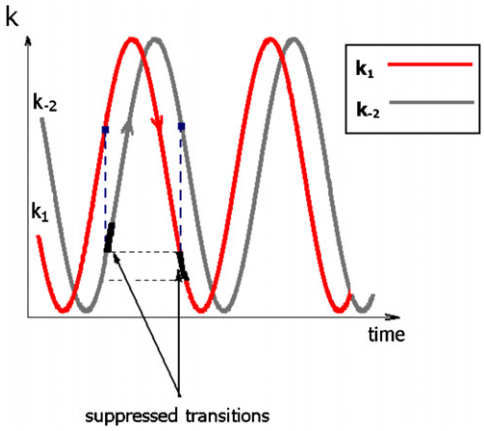

Figure 7. Illustration of the shielding mechanism of the SPE.

The following explicit expression for $F_{k_1,k_{-2}}$ is then obtained [100] by computing the eigenvectors of the Hamiltonian (32):

$$F_{k_1,k_{-2}} = \frac{e_{-\chi}(e^{i\chi}k_2 + k_{-1})}{[4\kappa_+ e_\chi + 4\kappa_- e_{-\chi} + K^2]^{3/2}}. \tag{39}$$

The generating function (34) contains information both about average flux and about flux fluctuations. To extract the average current from expressions (36) and (35) one should write the cumulant generating function as a power series in the small parameter χ and retain the linear part, namely

$$S_{\text{dyn}} \approx iS^{(1)}_{\text{dyn}}\chi + O(\chi^2), \qquad S_{\text{geom}} = i\chi \iint_{\mathbf{s_c}} dk_1\, dk_{-2} F^{(1)}_{k_1,k_{-2}} + O(\chi^2). \tag{40}$$

Higher order terms in χ can reveal information about the higher cumulants of stochastic fluxes, while the first-order terms coincide, up to $i\chi$, with the average number of transferred particles. For the process in figure 6, such calculations lead to the following expression [100] for the mean $S \to P$ flux per cycle:

$$J = J_{\text{geom}} + J_{\text{dyn}}, \tag{41}$$

$$J_{\text{geom}} = \iint_{\mathbf{s_c}} d^2k \frac{k_2 + k_{-1}}{K^3}, \tag{42}$$

$$J_{\text{dyn}} = \int_0^T dt \frac{\kappa_+(t) - \kappa_-(t)}{K(t)}. \tag{43}$$

It turns out that the dynamic contribution J_{dyn} to the current is just the steady-state current averaged over time. Equations (42) and (43) show that the geometric contribution J_{geom} to the current has strikingly different properties from the dynamic one. In fact, it does not have an analogue in a strict steady-state situation because it is nonzero only if the contour encloses a finite area in the parameter space, i.e. in order to make it nonzero, at least two parameters should be time dependent with a phase shift different from 0 or π. Another interesting property is that this contribution changes sign when the direction of motion along the contour is reversed.

An intuitive explanation of the phenomenon of $J_{\text{geom}} \neq 0$ is illustrated in figure 7. During an interval of time in which a molecule is bound to the enzyme, the bin of figure 6 is occupied

and the values of k_1 and k_{-2} have no effect on the system. If the left binding rate k_1 is higher than the right one k_{-2} during the upswing of the cycle, then k_1 'shields' growing values of k_{-2} from having an effect, while k_{-2} shields decreasing values of k_1 during the downswing. This leads to a phase-dependent asymmetry which is the source of the geometric pump flux.

It is instructive to compare the relation of the geometric phase (36) to the value given by equation (13) in the formalism of Landsberg–Ning–Haken, which was discussed in section 3. The pump current (41) itself can alternatively be derived directly from the master equation for the vector $\mathbf{p} = (p_{ES}, p_E)$ of probabilities of the enzyme (bin) states. These equations have the form

$$\dot{\mathbf{p}} = \hat{H}(\chi = 0, \mathbf{k})\mathbf{p}, \qquad \dot{N}_{\mathrm{P}} = J(\mathbf{p}, \mathbf{k}), \tag{44}$$

where N_{P} is the average number of product molecules created, and where the current $J(\mathbf{p}, \mathbf{k})$ is defined by

$$J(\mathbf{p}, \mathbf{k}) = p_{SE}k_2 - p_E k_{-2}. \tag{45}$$

This set of equations has the form (13), namely, probabilities relax to unique steady-state values at given rate constants $\mathbf{k}$, independently of the additional equation for N_{P}. The geometric phase (36), however, contains complete information about the stochastic evolution, including geometric contributions to higher cumulants, which cannot be derived from a set of equations in (44). The additional information provided by (35) and (36), but not by (44), is sometimes necessary. For example, it is needed for a complete description of counting statistics of currents in nanoscale electronic circuits, which were measured experimentally in [105]. The higher cumulants are also needed to account for contributions to particle fluxes due to stochastic transitions over potential barriers, as studied in [106, 107]. Thus the full stochastic treatment of such processes, beyond the formalism of equations (44), is inevitable, and the geometric contribution to higher cumulants has important consequences in the theory of such effects.

6. Non-cyclic geometric phase

The quantum-mechanical Berry phase can be extended to noncyclic evolution [108, 109]. Sinitsyn and Nemenman [110] showed that a moment generating function of the form (33) can be partitioned into geometric and dynamic parts even if the parameters change along an open circuit. For evolution during time δt we have

$$Z(\chi, \delta t) = \mathrm{e}^{S_{\mathrm{geom}}(\chi,\delta t)+S_{\mathrm{dyn}}(\chi,\delta t)}, \tag{46}$$

where $S_{\mathrm{dyn}} = \int_0^{\delta t} \mathrm{d}t\, \varepsilon_0(\chi, t)$ is the quasi-stationary part of the generating function and where

$$S_{\mathrm{geom}} = \int_{\mathbf{c}} [\mathbf{P}(\mathbf{k}) - \mathbf{A}(\mathbf{k})] \cdot \mathrm{d}\mathbf{k}, \tag{47}$$

with

$$\mathbf{P} = \partial_{\mathbf{k}} \ln\langle 1|u_0\rangle, \qquad \mathbf{A}(\mathbf{k}) = \langle u_0|\partial_{\mathbf{k}} u_0\rangle, \tag{48}$$

where $\langle 1| = (1, 1)$ is the vector with all unit entries. The noncyclic geometric phase contribution has no analogue in a strict steady-state regime. In general, for a non-cyclic evolution, the term $-\int_{\mathbf{c}} \mathbf{A}(\mathbf{k}) \cdot \mathrm{d}\mathbf{k}$ is not gauge invariant, and the term $\int_{\mathbf{c}} \mathbf{P}(\mathbf{k}) \cdot \mathrm{d}\mathbf{k}$ is a necessary correction to make it so. The integral over the additional vector $\mathbf{P}$ exactly cancels the non-gauge-invariant part of the contour integral of $\mathbf{A}$. The vector $\mathbf{P}$ introduces the gauge, which

can be derived from proper accounting for the effect of the averaging over the final states of the bin system at the end of the evolution.

Since **P** is an exact differential, it is important only when looking at an evolution along an open path in the parameter space. If the parameter vector **k** returns to its initial value at the end of the evolution, expression (36) becomes equivalent to the cyclic geometric phase defined in [100]. The origin of the gauge invariance of expression (47) can be traced from the Markovian property of the process. The gauge transformation

$$Z(\chi) \to Z(\chi)\, \mathrm{e}^{S_{\mathrm{prior}}(\chi)} \tag{49}$$

has the physical meaning of the assumption that additional currents, described by the cumulant generating function $S_{\mathrm{prior}}(\chi)$, have passed through the system before the time moment $t = 0$. In Markovian evolution, the currents counted after $t = 0$ should be independent of the currents counted prior to this moment, which means that expression (47), describing the currents after $t = 0$, is invariant of the gauge transformation (49).

7. Elimination of fast variables in stochastic processes

This section is technically more involved than the rest of the review, and can be safely omitted on a first reading. It contains a discussion of the method of stochastic path integral. This is a powerful technique for investigating stochastic fluxes in mesoscopic interacting systems. The discussion in section 5 reduces the problem of computing the counting statistics to that of finding eigenvalues and eigenvectors of a non-Hermitian Hamiltonian. This straightforward approach becomes extremely complicated when applied to complex systems with a mesoscopically large phase space. In contrast, the stochastic path integral technique allows us to derive moment generating functions of fluxes even in many-body interacting mesoscopic stochastic systems. We advise the reader, who is not familiar with stochastic path integrals, to study look at the articles [111–113] before reading this section. Sinitsyn and Nemenman [101] demonstrated that this technique can be applied to study geometric phases in the evolution of driven mesoscopic stochastic systems. In this section we discuss another application of geometric phases and the stochastic path integral, namely, to the problem of coarse graining stochastic kinetics.

Berry phases often appear in quantum-mechanical applications when one attempts to eliminate fast degrees of freedom and reduce a problem to an effective one which includes only slow variables. Such an approach is known as the *Born–Oppenheimer approximation* and has been very successful for describing near-equilibrium properties of most molecules. According to it, initially one solves a much simpler Schrödinger equation for electrons, treating nuclear degrees of freedom as adiabatically slowly changing parameters. After this, one assumes that the nuclei move on a single potential-energy surface created by the faster moving electrons. An interesting development involving this approach was the observation that the Berry phase, acquired by electronic wavefunction in a potential of slowly moving nuclei, influences the dynamics of slow degrees of freedom [2, 19, 114].

The evolution equations for moment generating functions in stochastic processes are similar to the quantum-mechanical Schrödinger equation [111]. We already encountered this analogy in section 5. This mathematical similarity was also used, for example, to study counting statistics in electronic transport [112, 113, 115], to estimate over-barrier escape probabilities [106, 107] and to classify stochastic phase transitions [116]. Many of the applications of this approach were restricted to relatively simple systems with only a few interacting species because quantum-mechanical equations are usually no simpler to investigate than the stochastic ones.

Recently, a stochastic-quantum analogy was proposed to simulate the behavior of large stochastic networks of biochemical reactions. In general, these networks involve many different chemical species and reaction types. [117]. One of the difficulties in studying such networks is their *stiffness*, i.e. strong timescale separation of various processes in a network. In its application to stochastic processes, the Born–Oppenheimer approximation rigorously captures statistical characteristics of chemical processes at coarse-grained scales [117].

In this section, we present a simple example of how a reduction of a model can be achieved and how geometric phases influence the evolution of slow variables. For this purpose we again consider the Michaelis–Menten type of conversion of S into P via creation of a substrate–enzyme complex, which we studied in section 5. Now, however, we assume that numbers of substrate and product molecules (N_S and N_P respectively) are independent dynamic variables, subject to all the conservation laws imposed by the given kinetic scheme. We also assume that the enzyme–substrate complex is created from substrate and product molecules at kinetic rates which are respectively proportional to the absolute numbers N_S and N_P of these molecules. We then have to consider the following four reactions:

(i) forward substrate–enzyme complex formation, $S + E \to SE$, with rate $k_1 N_S$;
(ii) backward substrate–enzyme complex formation, $P + E \to SE$, with rate $k_{-2} N_P$;
(iii) complex backward decay, $SE \to S + E$, with rate k_{-1};
(iv) product emission $SE \to E + P$, with rate k_2.

Since we have only one enzyme molecule but $N_S, N_P \gg 1$, it takes many identical steps for the enzyme molecule to convert a substantial number of substrates into products. This creates a timescale separation, which can be used to reduce the model to an effective process

$$S \to P. \tag{50}$$

Our goal is to find the statistical characteristics of the coarse-grained reaction (50). Let $T_{S\to P}$ be the time it takes an enzyme molecule to convert a substrate molecule to a product molecule. We choose a timescale δt which is much larger than $T_{S\to P}$, but much smaller than $N_S T_{S\to P}$. Suppose that we are looking for the moment generating function of the number n_P of product molecules created during a relatively long time $T \gg \delta t$:

$$\mathcal{Z}(\chi_C) = e^{\mathcal{S}(\chi_C)} = \sum_{n_P=-\infty}^{\infty} P(n_P|T)\, e^{i n_P \chi_C}. \tag{51}$$

Here we introduce an additional index C to mark a counting parameter in (51) in order to distinguish it from other variables which will appear in the following calculations. As noted in [111, 112], if one knows the statistical properties of fluxes at timescales δt then the moment generating function at larger timescales can be written in the form of a stochastic path integral. We will derive the stochastic path integral representation of the generating function in (51).

In sections 5 and 6 we already found the full counting statistics of the fluxes in the Michaelis–Menten model with slowly time-dependent parameters. To apply it to our model we should redefine kinetic rates as $k_1 \to k_1 N_S(t)$ and $k_{-2} \to k_{-2} N_P(t)$. This does not solve our problem completely, because at this stage we do not know the explicit time dependence of $N_S(t)$ and $N_P(t)$, which we regard as slow but dynamic variables. Let us partition the time line into intervals $(t_m, t_m + \delta t)$ of durations δt, where $t_m = m\delta t$, and let $\delta n_P(t_m)$ be the relative change in the number of product molecules during these time intervals. We chose δt sufficiently small, so that $\langle \delta n_P(t_m) \rangle / N_{P/S}(t_m) \ll 1$ while the absolute change is

large $\langle \delta n_{\rm P}(t_m)\rangle \gg 1$. The probability distributions of $\delta n_{\rm P}(t_m)$ are then given by the inverse Fourier transforms of the corresponding moment generating functions in section 6:

$$P(\delta n_{\rm P}(t_m)) = \int_{-\pi}^{\pi} \frac{d\chi(t_m)}{2\pi} \exp(-{\rm i}\chi(t_m)\delta n_{\rm P}(t_m) + S_{\rm MM}(\chi(t_m), \delta t)). \tag{52}$$

Here, $S_{\rm MM} = S_{\rm geom} + S_{\rm dyn}$ is the cumulant generating function of the number of new product molecules which were generated during time δt. Treating $N_{\rm S/P}(t)$ as slow time-dependent parameters, one finds that $S_{\rm MM}$ is given by equation (46).

The moment generating function of the number of product molecules created during a large time interval $(0, T)$ is given by the sum over all possible paths in the space of dynamic variables $N_{\rm S}(t_m)$, $N_{\rm P}(t_m)$ and $\delta n_{\rm P}(t_m)$, weighted by the probabilities (52) and by delta-functions, which are responsible for conservation of the number of molecules,

$$\delta^m_{N_{\rm S}} = \delta(N_{\rm S}(t_{m+1}) - N_{\rm S}(t_m) + \delta n_{\rm P}(t_m)), \tag{53}$$

$$\delta^m_{N_{\rm P}} = \delta(N_{\rm P}(t_{m+1}) - N_{\rm P}(t_m) - \delta n_{\rm P}(t_m)). \tag{54}$$

We use delta-functions instead of Kronecker symbols because the assumption $N_{\rm S/P}, \delta n_{\rm P}(t_m) \gg 1$ allows us to treat $N_{\rm S/P}$ and $\delta n_{\rm P}$ as continuous variables. Using that $n_{\rm P} = \sum_{m=1}^{T/\delta t} \delta n_{\rm P}(t_m)$, the moment generating function of this number is a discrete path integral

$$\begin{aligned} Z(\chi_{\rm C}) &\equiv \langle {\rm e}^{{\rm i}\chi_C n_{\rm P}}\rangle \\ &= \prod_m \int {\rm d}N_{\rm S}(t_m)\, {\rm d}N_{\rm P}(t_m)\, {\rm d}(\delta n_{\rm P}(t_m))\, P[\delta n_{\rm P}(t_m)]\, {\rm e}^{{\rm i}\chi_C \delta n_{\rm P}(t_m)} \delta^m_{N_{\rm S}} \delta^m_{N_{\rm P}}. \end{aligned} \tag{55}$$

We rewrite the delta-functions in (52) as integrals over oscillating exponents

$$\delta^m_{N_{\rm S/P}} = \frac{1}{2\pi} \int_{-\pi}^{+\pi} d\chi_{\rm S/P}(t_m) \exp({\rm i}\chi_{\rm S/P}(t_m)[N_{\rm S/P}(t_{m+1}) - N_{\rm S/P}(t_m) \pm \delta n_{\rm P}(t_m)]),$$

and substitute the result into (55). After this, integrals over $\delta n_{\rm P}(t_m)$ produce new delta-functions, which are easily removed by integration over $\chi(t_m)$, leaving us only with a path integral over the slow variables $N_{\rm S/P}(t_m)$ and $\chi_{\rm S/P}(t_m)$. Taking a continuous limit, we have $N_{\rm S/P}(t_{m+1}) - N_{\rm S/P}(t_m) \to \dot N_{\rm S/P}(t)\, {\rm d}t$, and we can rewrite the moment generating function as a path integral involving only slow variables:

$$\langle {\rm e}^{{\rm i}\chi_C n_{\rm P}}\rangle = \int DN_{\rm S}(t) \int DN_{\rm P}(t) \int D\chi_{\rm S}(t) \int D\chi_{\rm P}(t)\, {\rm e}^{S(\chi_{\rm C}, T)}, \tag{56}$$

where $S(\chi_{\rm C}, T)$ can be partitioned into dynamic and geometric parts

$$S(\chi_{\rm C}, T) = S^{\rm dyn}(\chi_{\rm C}, T) + S^{\rm geom}(\chi_{\rm C}, T), \tag{57}$$

such that

$$S^{\rm geom} = -\int_{\mathbf{c}} [A_{N_{\rm S}} dN_{\rm S} + A_{N_{\rm P}} dN_{\rm P} + A_{\chi_{\rm S}} d\chi_{\rm S} + A_{\chi_{\rm P}} d\chi_{\rm P}], \tag{58}$$

$$A_x = \langle u_0(\chi_{\rm S} - \chi_{\rm P} + \chi_C)|\partial_x|u_0(\chi_{\rm S} - \chi_{\rm P} + \chi_{\rm C})\rangle, \tag{59}$$

$$S^{\rm dyn} = \int_0^T {\rm d}t[{\rm i}\chi_{\rm S}\dot N_{\rm S} + {\rm i}\chi_{\rm P}\dot N_{\rm P} + H_{\rm MM}(N_{\rm S}, N_p, \chi_{\rm S} - \chi_{\rm P} + \chi_{\rm C})], \tag{60}$$

where $\mathbf{c}$ is the contour of the trajectory in the slow parameter space, x belongs to the set $\{N_{\rm S}, N_{\rm P}, \chi_{\rm S}, \chi_{\rm P}\}$ and $H_{\rm MM}$ plays the role of the effective Hamiltonian

$$H_{\rm MM} = \frac{K - \sqrt{K^2 + 4[N_{\rm S}k_1k_2({\rm e}^{{\rm i}(\chi_{\rm S}-\chi_{\rm P}+\chi_{\rm C})} - 1) + N_{\rm P}k_{-1}k_{-2}({\rm e}^{-{\rm i}(\chi_{\rm S}-\chi_{\rm P}+\chi_{\rm C})} - 1)]}}{2},$$

where $K \equiv k_1 N_S + k_{-2} N_P + k_{-1} + k_2$. This Hamiltonian is different from what one would expect if the conversion of S into P were a Poisson process, which reflects the non-Poisson nature of enzyme mediated fluxes. The geometric part of the action (58) is the result of the pump fluxes.

The path integral (56) is a formal solution of the problem of removing of fast degrees of freedom: it expresses the moment generating function in terms of only slow variables N_S, N_P, χ_S, χ_P and does not depend on the degrees of freedom of the enzyme.

Since the averages $\langle N_S \rangle$ and $\langle N_P \rangle$ are assumed large, one can use the saddle point solution of the path integral to derive semiclassical equations of motion for slow variables. Varying the action results in four coupled differential equations

$$\mathrm{i}\dot{N}_S = -\frac{\partial H_{MM}}{\partial \chi_S} - \mathrm{i}F_{\chi_S,N_S}\dot{N}_S - \mathrm{i}F_{\chi_S N_P}\dot{N}_P, \tag{61}$$

$$\mathrm{i}\dot{N}_P = -\frac{\partial H_{MM}}{\partial \chi_P} + \mathrm{i}F_{\chi_S,N_S}\dot{N}_S + \mathrm{i}F_{\chi_S N_P}\dot{N}_P, \tag{62}$$

$$\mathrm{i}\dot{\chi}_S = \frac{\partial H_{MM}}{\partial N_S} - \mathrm{i}F_{\chi_S,N_S}\dot{\chi}_S - \mathrm{i}F_{\chi_S N_P}\dot{\chi}_P + \mathrm{i}F_{N_S,N_P}\dot{N}_P, \tag{63}$$

$$\mathrm{i}\dot{\chi}_P = \frac{\partial H_{MM}}{\partial N_P} + \mathrm{i}F_{\chi_S,N_S}\dot{\chi}_S + \mathrm{i}F_{\chi_S N_P}\dot{\chi}_P - \mathrm{i}F_{N_S,N_P}\dot{N}_S, \tag{64}$$

where $F_{x_1,x_2} = \mathrm{i}(\partial A_{x_2}/\partial x_1 - \partial A_{x_1}/\partial x_2)$ and we used that A_{x_m} depends on χ_S, χ_P via the combination $(\chi_S - \chi_P)$ which leads to the relations $F_{\chi_n,\chi_m} = 0$, $F_{\chi_S,N_S} = -F_{\chi_P,N_S}$ and $F_{\chi_S,N_P} = -F_{\chi_P,N_P}$. The boundary conditions can be also influenced by geometric phases and should be derived by the method used in [111, 112].

For $\chi_C = 0$ there is a solution to equations (64) such that $\chi_S = \chi_P = 0$. N_S, N_P then satisfy coupled equations, which are known to coincide with the mean field equations [112]

$$\mathrm{i}\dot{N}_S = -\mathrm{i}\Omega_{\chi_S,N_S}\dot{N}_S - \mathrm{i}\Omega_{\chi_S N_P}\dot{N}_P - \left.\frac{\partial H_{MM}}{\partial \chi_S}\right|_{\chi_S=\chi_P=\chi_C=0}, \tag{65}$$

$$\mathrm{i}\dot{N}_P = \mathrm{i}\Omega_{\chi_S,N_S}\dot{N}_S + \mathrm{i}\Omega_{\chi_S N_P}\dot{N}_P - \left.\frac{\partial H_{MM}}{\partial \chi_P}\right|_{\chi_S=\chi_P=\chi_C=0}, \tag{66}$$

where $\Omega_{x_1,x_2} = F_{x_1,x_2}|_{\chi_S=\chi_P=\chi_C=0}$. Explicitly, for our model one can find that

$$\Omega_{\chi_S,N_S} = -k_1(k_2 + k_{-1})\frac{(k_2 + k_{-2}N_P)}{K^3}, \tag{67}$$

$$\Omega_{\chi_S,N_P} = -k_{-2}(k_2 + k_{-1})\frac{(k_2 + k_{-2}N_P)}{K^3}. \tag{68}$$

If substrate and product have no other dynamics than the conversion into each other via the ES complex, then $\dot{N}_P = -\dot{N}_S$ and

$$\left.\frac{\partial H_{MM}}{\partial \chi_S}\right|_{\chi_S=\chi_P=\chi_C=0} = -\left.\frac{\partial H_{MM}}{\partial \chi_P}\right|_{\chi_S=\chi_P=\chi_C=0} = \mathrm{i}(k_1 k_2 N_S - k_{-1}k_{-2}N_P)/K,$$

so, the evolution equation (66) for N_P becomes

$$\dot{N}_P = \frac{(k_1 k_2 N_S - k_{-1}k_{-2}N_P)}{K} - \frac{(k_2 + k_{-1})(k_1\dot{N}_S + k_{-2}\dot{N}_P)(k_2 + k_{-2}N_P)}{K^3}. \tag{69}$$

The first term in (69) is the usual quasi-steady-state prediction for the substrate-product conversion rate, and the second term is a correction due to the geometric phase contribution to the effective action. We note again that equations (64) contain information both about average fluxes and their fluctuations, while the result (69) is equivalent to the mean-field prediction for the average number of N_P. Substituting the solution of (64) into (57), one obtains the full counting statistics of the number n_P of product molecules created.

Terms resembling the geometric phase corrections in (64) also appear naturally in variational approaches to chemical kinetics [118]. Equations of motion, such as (64) are known in condensed matter physics, where similar Berry phase terms lead to distinct effects, such as the anomalous and the spin Hall effects [7–9]. Generally, the geometric phase correction in (69) is smaller than the quasi-steady-state part. However, there are situations when it can be important due to its specific symmetries [110].

8. Driven limit cycle

An interesting geometric phase was found by Kagan *et al* [119] in dissipative systems evolving to a limit cycle. In addition to a geometric phase that appears after the elimination of quickly decaying modes, they found also a geometric phase which arises from the nontrivial topology of the limit cycle itself. Consider the following evolution equation:

$$\frac{\mathrm{d}\phi}{\mathrm{d}t} = \Omega(\phi, \mu), \tag{70}$$

where $\Omega(\phi) = \Omega(\phi + 2\pi)$ is the instantaneous frequency and μ is a vector of internal parameters, which is slowly and periodically time dependent. Since the evolution is periodic, we can regard ϕ as a phase. Introducing the new variable

$$\theta(\phi, \mu) = \int_0^{\phi} \frac{\omega(\mu)}{\Omega(\phi', \mu)}\,\mathrm{d}\phi', \tag{71}$$

which is a rescaled version of ϕ, defined so that θ evolves at the constant rate

$$\omega(\mu) = \left(\frac{1}{2\pi}\int_0^{2\pi} \frac{1}{\Omega(\phi', \mu)}\,\mathrm{d}\phi'\right)^{-1} \tag{72}$$

when μ is fixed, Kagan *et al* showed that for adiabatic cyclic evolution of μ the phase (71) becomes the sum of dynamic and geometric parts,

$$\theta(T) = \theta_{\mathrm{dyn}}(T) + \theta_{\mathrm{geom}}(T), \tag{73}$$

where T is the period of the adiabatic evolution of parameters,

$$\theta_{\mathrm{dyn}}(T) = \int_0^T \mathrm{d}t\,\omega(\mu(t)) \tag{74}$$

and

$$\theta_{\mathrm{geom}}(T) = \oint \mathbf{A}\cdot\mathrm{d}\mu, \tag{75}$$

where

$$\mathbf{A} = \int_0^{2\pi} \frac{\mathrm{d}\phi}{2\pi}\left[\frac{\omega(\mu)}{\Omega(\phi, \mu)}\partial_\mu\theta(\phi, \mu))\right]. \tag{76}$$

One can look at the geometric phase (75) from the point of view of the stochastic path integral representation, which was discussed in section 7. As in the derivation of the stochastic

path integral, one can promote the evolution (70) to a Hamiltonian flow by introducing a variable Λ, which is canonically conjugate to ϕ, with the Hamiltonian

$$H(\Lambda, \phi) = \Lambda\Omega(\phi, \mu). \tag{77}$$

The phase evolution (70) then follows from the canonical equation

$$\frac{\mathrm{d}\phi}{\mathrm{d}t} = \frac{\partial H}{\partial \Lambda}. \tag{78}$$

Sinitsyn and Ohkubo [120] showed that, in this Hamiltonian evolution, θ_{geom} becomes a Hannay angle [33], which is a geometric phase in classical mechanics that is responsible for the rotation of the Foucault pendulum, and many other subtle effects.

9. Thermodynamic constraints and geometric phases

Geometric approach to classical thermodynamics began with Josiah Willard Gibbs' pioneering work, called 'Graphical Methods in the Thermodynamics of Fluids' [121]. With the development of this point of view, it has become possible to formulate classical equilibrium and near-equilibrium thermodynamics in terms of the theory of metric spaces and the vector geometry [122].

Many applications of geometric phases in stochastic kinetics involve perturbation of systems initially in thermodynamic equilibrium. These include the response of molecular motors or mesoscopic electronic circuits to periodic evolution of parameters. The laws of thermodynamics impose constraints on the kinetic rates which guarantee that the Boltzmann distribution at a given temperature describes the equilibrium state. These constrains also have important consequences for geometric phases.

Were it not for geometric phases, a thermodynamic system with adiabatically changing parameters would have no average current. When detailed balance conditions are imposed on kinetic rates at any moment of time, a strict quasi-steady-state approximation predicts exactly zero fluxes on average in response to adiabatically slow perturbations. Hence, the geometric phase is the only mechanism that can be responsible for nonzero currents in such systems. In this section, we discuss several examples in support of this conclusion.

9.1. Reversible ratchet

Ratchets are systems, where particles diffuse in a potential, which is periodic both in space and time, i.e. $V(x, t) = V(x + L, t) = V(x, t + T)$. The particle distribution $\rho(x, t)$ satisfies the Fokker–Planck equation, which predicts that for a fixed potential profile, $\rho(x, t)$ relaxes to the Boltzmann distribution $\rho(x) = C\mathrm{e}^{-V(x)/k_BT}$, where C is a normalization constant. An example of a ratchet is shown in figure 8. The ratchet working in the regime of adiabatically slow evolution of the potential profile is called the *reversible ratchet* because currents in this limit change sign when the potential profile changes with time in a reversed order. Thus, the reversible ratchet is a simple example of a device working near thermodynamic equilibrium.

Currents in a discrete version of a reversible ratchet were studied by Markin and Astumian [123]. The continuous model [124] was studied by Parrondo, who derived the explicit expression for the current of particles in such a system in the limit of adiabatically slow changes of the potential. The paradox is that, for adiabatically slow changes, one can expect that the particle distribution would have enough time to converge to an instantaneous equilibrium distribution, i.e. it is expected to have a form $\rho(x, t) \approx C(t)\,\mathrm{e}^{-V(x,t)/k_BT}$. Such a varying Boltzmann distribution does not predict any current on average in the system at any moment of time, while apparently the solution of the problem predicts a nonzero current. Sinitsyn and

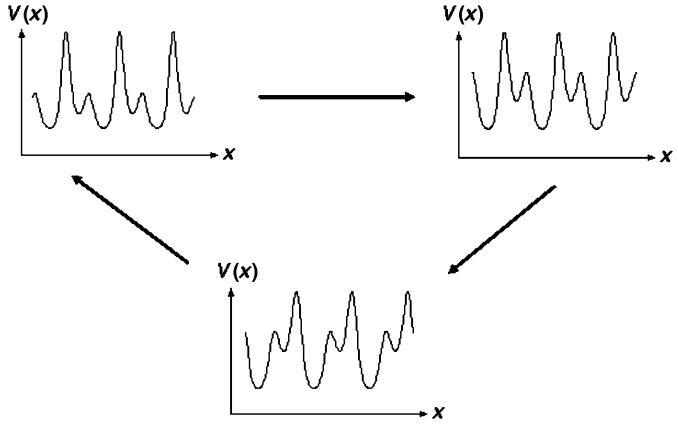

Figure 8. Snapshots of a ratchet potential at three stages of its evolution.

Nemenman [101] explored this model from the point of view of the stochastic path integral representation of the moment generating function of particle currents $Z(\chi, T)$. They showed that

$$Z(\chi, T) = \mathrm{e}^{\mathrm{i}\chi \oint_{\mathbf{c}} \mathbf{A}(\mathbf{k})\cdot \mathrm{d}\mathbf{k} + O(\chi^2)}, \tag{79}$$

where $\mathbf{k}$ is the vector of parameters controlling the shape of $V(x)$ and $\mathbf{c}$ is the contour in this parameter space. According to (79), the geometric phase is not zero, and contributes to the linear term in χ of the moment generating function. This confirms that the current in an adiabatic reversible ratchet is nonzero and arises purely geometrically. It can be totally controlled by choosing a proper contour in the space of potential shapes.

An interesting observation about this effect was made by Shi and Niu [125], who showed that this current can be quantized and that this quantization can be related to a Chern number of a Bloch band related to the periodic potential.

9.2. Geometric phases and fluctuation-dissipation relations

The adiabatic SPE appears when two time-dependent periodic perturbations are applied. From the discussion in section 5, it follows that the average flux of the 'charge', pumped by an application of infinitesimal cyclic external fields $h_B(t)$ and $h_C(t)$, is proportional to the area inside the contour of parameter evolution. We also showed that the pump current reverses its sign when a system is moving along the same contour but in the opposite direction. This situation can be expressed as the following law,

$$\delta q = F_{BC}\, \mathrm{d}h_B \wedge \mathrm{d}h_C, \tag{80}$$

where δq is the average of the flux that passes through the system during one cycle of the adiabatic periodic evolution, $\mathrm{d}h_B \wedge \mathrm{d}h_C$ is the infinitesimal directed area enclosed by the contour in the space of control parameters, and F_{BC} is the proportionality coefficient which, up to an $\mathrm{i}\chi$-factor, coincides with the part of the Berry curvature linear in χ.

According to the fluctuation–dissipation theorem [126], some transport coefficients near the point of thermodynamic equilibrium can be expressed in terms of correlation functions at the equilibrium point. Relations of this kind tell us a lot about the coefficient F_{BC} [90, 127]. The quantum version of the adiabatic pump effect can be quantified using the

Kubo formula [90]. One can derive the analogous result for a classical stochastic pump, operating near thermodynamic equilibrium, using a classical version of linear response theory [128].

Assume that the variables B and C coupled to the fields h_B and h_C in expression for the thermodynamic potential are invariant under time reversal. Then at the thermodynamic equilibrium, with fixed h_B and h_C, all currents are zero on average, that is

$$\langle J(t)\rangle_{h_B,h_C} = 0, \tag{81}$$

where $\langle\cdots\rangle_{h_B h_C}$ denotes the average over the equilibrium distribution at given values of h_B and h_C. If we start at equilibrium and increase h_B, h_C by small amounts δh_B and δh_C, then $h_\alpha(t) = h_\alpha(0) + \delta h_\alpha \theta(t)$, where $\alpha = B, C$. According to linear response theory, the current at a moment $t > 0$ is given by

$$J(t) = \delta J_B(t) + \delta J_C(t), \tag{82}$$

where

$$\delta J_\alpha(t) = 2\mathrm{i}\int_0^t \mathrm{d}t'\,\chi''_{J\alpha}(t-t')\delta h_\alpha, \tag{83}$$

and $\chi''_{J\alpha}(\omega)$ is the response function [126]. Letting $\chi''_{J,\alpha}(\omega)$ be the Fourier transform of $\chi''_{J,\alpha}(t)$, we then have

$$\delta J_\alpha(t) = \int \frac{\mathrm{d}\omega}{2\pi}\frac{2\delta h_\alpha \chi''_{J\alpha}(\omega)}{\omega}\,\mathrm{e}^{\mathrm{i}\omega t}. \tag{84}$$

Here, we have used the fact that J and B (resp. C) have different time reversal properties so that the static susceptibility [126] is identically zero, i.e.

$$\int \frac{\mathrm{d}\omega}{2\pi}\frac{\chi''_{J\alpha}(\omega)}{\omega} = 0. \tag{85}$$

The classical *fluctuation–dissipation theorem* [126] states that

$$\chi''_{J\alpha}(\omega) = \frac{\beta\omega}{2} S_{J\alpha}(\omega), \qquad \beta = 1/k_{\mathrm{B}}T, \tag{86}$$

where $S_{J\alpha}(\omega)$ is the Fourier transform of the correlator

$$S_{J\alpha}(t-t') = \langle J(t)\alpha(t')\rangle, \qquad \alpha = B, C \tag{87}$$

at equilibrium. Substituting (86) and (87) into (84) and integrating over time, the total flux δq passed due to a perturbation is

$$\delta q = Q_{JB}\delta h_B + Q_{JC}\delta h_C, \tag{88}$$

where

$$Q_{JB} = \beta\int_0^\infty \mathrm{d}t\, S_{JB}(t), \tag{89}$$

$$Q_{JC} = \beta\int_0^\infty \mathrm{d}t\, S_{JC}(t). \tag{90}$$

Note that both Q_{JB} and Q_{JC} are completely determined by the equilibrium correlation functions for nonzero B and C. If we imagine that the adiabatic evolution in the space of control parameters consists of small perturbations, as above, then the total transferred charge after one cycle is

$$\delta q = \oint_{\mathbf{c}} \{Q_{JB}\mathrm{d}h_B + Q_{JC}\mathrm{d}h_C\} = \iint_{\mathbf{s_c}} \mathrm{d}h_B \wedge \mathrm{d}h_C F_{BC}, \tag{91}$$

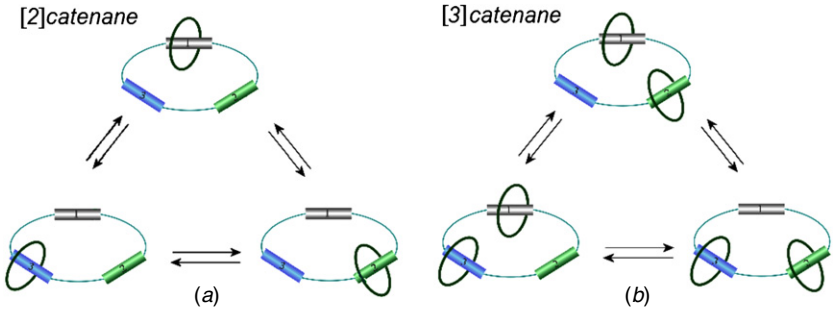

Figure 9. Topology and metastable states of (a) [2]catenane and (b) [3]catenane molecules. Smaller rings are capable to perform directed rotational motion around the larger ring in response to external periodic driving. In [3]catenanes, unlike [2]catenanes, directed motion can be achieved even when only coupling strengths of smaller rings to the three stations on the larger ring are controlled.

where **c** is the contour in the space of control parameters and F_{BC} is the transport coefficient that we have been looking for. According to Stokes' theorem

$$F_{BC}(h_B, h_C) = \frac{\partial Q_{JC}}{\partial h_B} - \frac{\partial Q_{JB}}{\partial h_C}. \tag{92}$$

Equation (92) shows that the pump transport coefficient can be expressed as the circulation, in the space of controlled parameters, of a vector **Q** whose components are the values of the correlators (89) and (90) at equilibrium. Such relations indicate that the ability of a system to perform as a stochastic pump in response to periodic perturbations, can be inferred, in principle, from system properties at thermodynamic equilibrium. This can lead to simplifications during numerical or perturbative analysis of molecular motor operations, because the equilibrium properties are relatively easy to investigate. For example, calculations of free energy landscapes are achievable for complex biological molecules such as the kinesin molecular motor [129].

9.3. Beyond adiabatic and perturbative limits

So far, we have only discussed the systems, which are driven adiabatically slowly. Quantum-mechanical Berry phase can be generalized to the case of non-adiabatic evolution [108]. Following this analogy, Ohkubo showed that geometric phases in stochastic kinetics also can be considered in the non-adiabatic regime [99].

Recently, a number of exact results in the theory of the stochastic pump effect were derived which are valid in nonperturbative and nonadiabatic regimes [130, 131]. These results were motivated partly by recent experiments with [2]- and [3]catenane molecules [133–135]. Such molecules are made of interlocked rings, as shown in figure 9 ([n]catenane is made of n rings.). By changing external conditions periodically, one can modulate the coupling strengths of smaller rings to special sites (stations) on the larger ring to force the smaller ones to orbit around the center of the larger ring while remaining interlocked with it. Astumian showed in [136] that adiabatic modulation of couplings to stations cannot be used to select a preferred mean orientation (clockwise or counterclockwise) of the orbit of the small ring in [2]catenane about the large ring, but can be used to select a preferred mean orientation for the orbit of the pair of small rings around the large ring in a [3]catenane in figure 9.

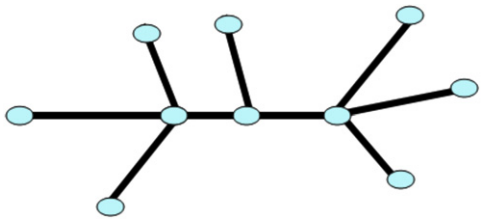

Figure 10. A graph with a tree-like topology.

Any finite Markov chain can be represented as a graph. In such a graph, vertices correspond to discrete states of a system and links correspond to allowed transitions. We say that kinetic rates k_{ji} of transitions from the state i to the state j satisfy the *detailed balance condition* if they can be parametrized by parameters E_i (called *well depths*) and $W_{ij} = W_{ji}$ (called *barrier heights*) such that $k_{ji} = k \exp[E_i - W_{ij}]$. The detailed balance conditions guarantee that if all parameters are time independent then the state probability vector relaxes to a Boltzmann distribution. Every vertex in a graph, representing a Markov chain, is associated with parameter E_i and every link corresponds to some finite W_{ij}.

Rahav *et al* [130] showed that the result observed in catenane molecules is a consequence of a much more general *no-pumping theorem*. They showed that for a periodic *non-adiabatic* driving protocol, the average flux Q, passed through any link $i - j$ of a graph representing a finite Markov chain, can be written as a sum of geometric and dynamic parts, i.e.

$$Q = \int_0^T \mathrm{d}t\, J_{\mathrm{dyn}}(t) + \oint_{\mathbf{c}} \mathbf{A} \cdot \mathrm{d}\mathbf{p}. \tag{93}$$

In the first term in (93), T is the driving period. The second term in (93) is geometrical and depends only on the path $\mathbf{c}$ in the space of values of the state probability vector $\mathbf{p}$. The representation (93) is not an explicit solution because the evolution of the probability vector $\mathbf{p}$ is not assumed to be known. However, the authors of [130] showed that when detailed balance conditions are imposed, even on time-dependent kinetic rates, the dynamic part in (93) becomes identically zero. Thus, even for rapid variation of the control parameters, the flux is purely geometrical. Moreover, they showed that the connection $\mathbf{A}$ is independent of E_i. As a consequence, if some well depths E_i are varied, while W_{ij} remain fixed, and if the probability vector returns to the initial values at the end of the evolution, the geometric term becomes also zero because $\oint_{\mathbf{c}} \mathbf{A} \cdot \mathrm{d}\mathbf{p} = \mathbf{A} \cdot \oint_{\mathbf{c}} \mathrm{d}\mathbf{p} = 0$.

Chernyak and Sinitsyn [131] derived and proved the pumping-restriction theorem, which includes the no-pumping theorem of [130] as a special case. The *pumping-restriction theorem* makes two assertions. The first assertion tells us that not all pumped currents, i.e. time-averaged currents induced by a cyclic evolution of parameters, are independent. More precisely, pump currents through various links can be considered as vectors in a vector space whose dimension is equal to the maximum number of time-dependent barriers W_{ij} such that removing the links, corresponding to these barriers, does not break the graph into disjoint components. A trivial consequence of this theorem is that the pump current through any link on a tree-like graph, such as the one in figure 10, is exactly zero. Indeed, removing any link from a tree (not touching the vertices) breaks it into disjoint components, and according to the pumping-restriction theorem, the pump current on such a graph should be zero.

The result for a tree graph is expected because, for periodic evolution of parameters, the flux through any link on such a graph should eventually return through the same link moving in the opposite direction since initial and final state probability vectors coincide. Hence, the integrated current must be zero. The pumping-restriction theorem leads also to many

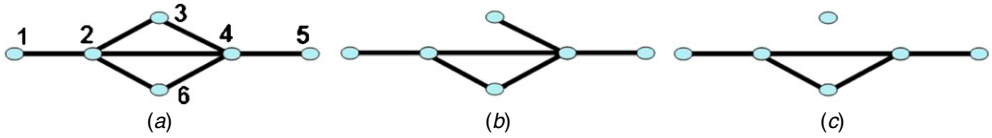

Figure 11. (*a*) A graph representing a six-state Markov chain. (*b*) Removing the link 2–3 alone does not break the graph into disjoint components. (*c*) Removing links 2–3 and 3–4 breaks the graph.

less obvious predictions. For example, in the graph in figure 11(*a*), one can, by perturbing periodically well depths E_i and also only the barriers related to links 2–3 and 3–4, induce a nonzero pump current, because removing any one of the links 2–3 or 3–4 does not break the graph into disjoint components, as is shown in figure 11(*b*). According to the theorem, however, a pump current through any link in figure 11(*a*) will then be proportional to the pump current through the link 2–3 with a constant proportionality coefficient because removing both links 2–3 and 3–4 we would break the graph into disjoint parts, as is shown in figure 11(*c*). Hence the dimension of the pump current space in this case is only 1. The pumping-restriction theorem also predicts that an arbitrary periodic driving of parameters on the links 1–2 and 4–5 in figure 11 alone cannot induce the pump effect, because removing any of those links would break the graph. That should suffice to explain and illustrate the first assertion of the pumping-restriction theorem. As for the second assertion of the theorem, it states that if pump currents are allowed, and if there are restrictions on their values predicted by the first part of the theorem, then these restrictions do not depend on parameters E_i.

The existence of exact results, such as the no-pumping and the pumping-restriction theorems, tells us that there are strong constraints which must be satisfied by control parameters in order to induce a directed motion of a nanoscale device. At this stage it is unclear whether these theorems can be extended to include current fluctuations, or whether the pumping-restriction theorem can be related to other exact results in non-equilibrium thermodynamics, such as the Jarzynski equality [137], or the invariant quantities in a shear flow found in [132]. We note that a number of fluctuation theorems have been found for applications to ratchet systems and molecular motors [138–143], but their connections to geometric phases are unknown.

10. Geometric phases and molecular motors

Applications of geometric phases in mathematical robotics are based on the same geometric structure as the one discussed by Shapire and Wilczek to describe the locomotion of living cells [71, 72]. As in the case of living organisms, the internal motions of robots are confined to a particular region as the robot performs its tasks. Nevertheless, as the robot interacts with its environment, periodic changes in the internal control variables can lead to nonperiodic effects on the robot position or on its surroundings. The reader is referred to [15, 144, 145] for an introduction to the geometric theory of robotic motion and for references to its extensive literature. In this section we demonstrate how geometric phases in stochastic kinetics appear in the control theory of the molecular machines.

Many biological molecules resemble motors, and sometimes operate according to principles similar to those which govern the macroscopic machines used by humans. Molecular motors are ubiquitous in living organisms. They are employed, for example, for transport, for injecting viruses into living cells, for unzipping the DNA and for storing energy [146, 147].

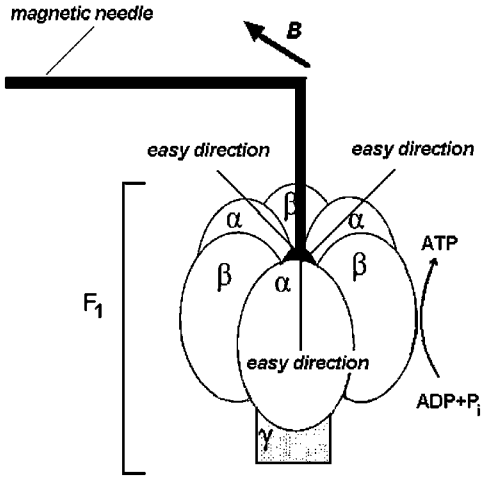

Figure 12. F_1-subunit of the natural molecular motor F_0F_1-ATPase with attached magnetic needle in external magnetic field **B**.

Experimental progress in the synthesis and observation of molecular motors has been remarkable. The reviews [148, 149] describe many recently synthesized molecules such as rotaxanes and catenanes, which are able to perform prescribed mechanical movements in response to external stimulus. Moreover, the experimental techniques for observing molecular motion have reached a level where discrete steps in a molecular motor operation can be observed [150, 151]. It has become feasible to measure noise and even the tails of the probability distributions of reaction events [150, 152, 153].

Better understanding of the working principles of nanoscale machines will make it possible to rebuild them to perform specialized tasks. In living cells, the molecular motor F_0 F_1-ATPase can convert the energy of an H^+ gradient into chemical energy stored in ATP. This natural molecular motor was rebuilt recently by modifying its F_1-subunit and was used to store the work done by an external magnetic field as chemical energy [154]. Another artificial modification of this molecular motor, shown in figure 12, was used in [155] to demonstrate the rotation of a metallic bar, powered by ATP.

At the molecular level, fluctuating forces are considerably stronger than typical external fields. Unlike macroscopic machines, molecular motors such as F_0F_1-ATPase absorb chemical energy in discrete portions and randomly. This leads to the so-called *shot noise* in their operations. Molecular motors are also affected by strong thermal fluctuations. These fluctuations are not merely a theoretical complication. For example, vesicle transport via the 'hitchhiking' mechanism, proposed in [156] depends on stochasticity in an essential way. Single molecule experiments show that noise measurements can provide important information about molecular structure [150] which can, in turn, be employed to uncover details of the working cycle of a molecular motor. Thus, the theory of molecular motor operations must take stochastic effects into account.

Much effort has been devoted to modeling the thermodynamics of molecular motors using the models of stochastic pumps and ratchets [84–87, 157]. This work has been reviewed in [158–161]. In contrast, appreciation of the role of geometric phases in molecular motor operations is relatively recent and is still in an early stage of development [100, 101, 124, 136, 162–164].

To illustrate that role, we consider a model inspired by the structure shown in figure 12, where the metallic bar is magnetic and the whole structure is placed in a rotating magnetic field. The molecule has an approximate three-fold symmetry (except for its rotating γ-subunit). If the magnetic coupling to the needle is weaker than the size of the potential barrier W between any pair of metastable states, the kinetics can be minimally described by a three-state model with some stochastic transition rates between any pair of neighboring states, as shown in figure 3. Near equilibrium, rotational steps of the γ-subunit in both directions were observed experimentally [165]. Due to the magnetic needle, it is possible to control the relative energies of the three states and of the potential barriers, which separate them, by applying an external rotating magnetic field. We will be interested in the number of full rotations of the needle, and hence of the γ-subunit attached to it, as it is driven in a neighborhood of thermodynamic equilibrium.

One can parametrize kinetic rates of an arbitrary Markov chain with detailed balance conditions in the following way, using the terminology 'well-depth' and 'barrier height' which was introduced in section 9.3: for sites i and j, the transition rate from j to i is $k_{ij} = k\,\mathrm{e}^{E_j - W_{ij}}$, where E_j is the well-depth j, and $W_{ij} = W_{ji}$ is the barrier height between sites i and j. Here, the energy scale is $k_B T = 1$, where T is temperature and k_B is the Boltzmann constant. The parameter k is a constant rate coefficient which sets the timescale and depends on the properties of the solution, i.e. on environment of the molecular motor. Imitating the procedure that was used in section 5, one finds that the moment generating function of the number of full rotations in the clockwise direction (counting counterclockwise rotations with a negative sign) is again given by equation (33), but with the new Hamiltonian that reads

$$\hat{H}(\chi) = \begin{pmatrix} -(k_{21}+k_{31}) & k_{12}\,\mathrm{e}^{-\mathrm{i}\chi/3} & k_{13}\,\mathrm{e}^{\mathrm{i}\chi/3} \\ k_{21}\,\mathrm{e}^{\mathrm{i}\chi/3} & -(k_{32}+k_{12}) & k_{23}\,\mathrm{e}^{-\mathrm{i}\chi/3} \\ k_{31}\,\mathrm{e}^{-\mathrm{i}\chi/3} & k_{32}\,\mathrm{e}^{\mathrm{i}\chi/3} & -(k_{13}+k_{23}) \end{pmatrix}. \tag{94}$$

The magnetic field modulates the parameters E_i and W_{ij}, and hence k_{ji}. The three-fold symmetry of the molecule can be taken into account by assuming the following dependence of the parameters E_i on the components B_x and B_y of the magnetic field:

$$\begin{aligned} E_1 &= b_y, \\ E_2 &= b_x \cos(\pi/6) - b_y \cos(\pi/3), \\ E_3 &= -b_x \cos(\pi/6) - b_y \cos(\pi/3), \end{aligned} \tag{95}$$

where $b_{x/y} = -B_{x/y}|\mathbf{M}|$ and $\mathbf{M}$ is the magnetization vector of the needle. One can derive (95) by assuming that the first metastable state corresponds to the magnetic bar pointing along y-axes and the other two are generated by a rotation of the needle by angles $2\pi/3$ and $4\pi/3$. For the magnetization energy ϵ, we use units where $\epsilon = -\mathbf{B}\cdot\mathbf{M}$. Suppose that the maxima of the potential barriers are shifted from the potential well minima by an angle ϕ. Thus a reasonable assumption for the dependence of the barrier heights on the magnetic field would be

$$\begin{aligned} W_{12} &= W + b_x \sin(\phi) + b_y \cos(\phi), \\ W_{23} &= W + b_x \cos(\pi/6 + \phi) - b_y \cos(\pi/3 - \phi), \\ W_{13} &= W - b_x \cos(\pi/6 - \phi) - b_y \cos(\pi/3 + \phi). \end{aligned} \tag{96}$$

According to the procedures of [100], which have been discussed in section 5, the moment generating function of the number of full rotations of the needle is determined by the eigenvalue with the lowest real part and corresponding eigenvectors of (94). While it is not convenient to study the exact expressions for eigenvectors of a 3×3 matrix, it is not hard to derive the lowest cumulants of the rotation numbers by treating the counting parameter χ perturbatively, as in

[166]. As in the example of the reversible ratchet, the principle of detailed balance imposes constraints which imply that, on average, the needle rotation becomes a purely geometric phase effect and that the average number of needle rotations per cycle can be expressed as an integral over a surface $\mathbf{S_c}$ whose boundary is the contour $\mathbf{c}$ in the (b_x, b_y) parameter space, namely

$$\langle n \rangle = \int\!\!\int_{\mathbf{S_c}} \mathrm{d}b_y \, \mathrm{d}b_x \, F(b_x, b_y). \tag{97}$$

The 'Berry curvature' $F(b_x, b_y)$ determines the sensitivity of the system to external driving forces. Regions with larger values of the function $F(b_x, b_y)$ correspond to parameter values at which system makes more rotations, on average, in response to periodic parameter variations. For a symmetric barrier configuration ($\phi = \pi/3$), the expression for $F(b_x, b_y)$ is particularly simple, namely

$$F(b_x, b_y) = \frac{3\sqrt{3}\,\mathrm{e}^{3\sqrt{3}b_x/2+3b_y}}{(\mathrm{e}^{\sqrt{3}b_x/2} + \mathrm{e}^{3b_y/2}(1 + \mathrm{e}^{\sqrt{3}b_x}))^3}. \tag{98}$$

Positivity of the Berry curvature in figure 13 means that the maximum number of rotations per one cycle is achieved for the contour that encloses the whole bright area in figure 13 from a very large distance in the parameter space. For any such a large contour, the result of the integration (97) of the Berry curvature remains approximately the same and can be estimated by setting the limits of the integration in (97) to infinities, which gives

$$\int_{-\infty}^{\infty}\int_{-\infty}^{\infty} \mathrm{d}b_y \, \mathrm{d}b_x \, F(b_x, b_y) = 1. \tag{99}$$

The result shows that the system in figure 12 makes, on average, at most one net rotation for every rotation of the magnetic field along a closed non-intersecting contour. This result does not require that the coupling to the magnetic field be the largest energy scale in the model. In our calculations we always assumed that $W > b_{x/y}$, in order to use a three-state approximation. The resulting quantization happens only on average, and the needle is allowed to make many stochastic steps before the rotation of the magnetic field is complete.

By comparing the number of rotations of the structure with the absolute value of the field, one can determine the function $F(b_x, b_y)$ experimentally. Figure 13 shows that $F(b_x, b_y)$ has the same three-fold symmetry as the kinetic model in figure 3. Its values can therefore reveal details of the internal molecular structure and of possible components in the effective kinetic model. Interestingly, the theory predicts that the geometric phase and the function in figure 13 are independent of the parameter k and of the size of an unperturbed barrier W. This means, in particular, that the function $F(b_x, b_y)$ can be robust against variations of the viscosity of the solution. This prediction is valid as long as the magnetic field rotation is adiabatically slow and the system always remains close to thermodynamic equilibrium. Thus we predict a universality of the motor response, in a sense that it does not depend on the solution viscosity, which can be tested experimentally. If the molecular motor is subject to additional forces, such as a proton gradient, which drive it beyond the regime of approximate thermodynamic equilibrium, this universality may no longer hold.

11. Discussion

The analogy between the evolution of generating functions in stochastic processes and the evolution of quantum-mechanical wavefunctions allows us to consider complex stochastic processes using the framework of quantum mechanics. In this review we discussed how, due

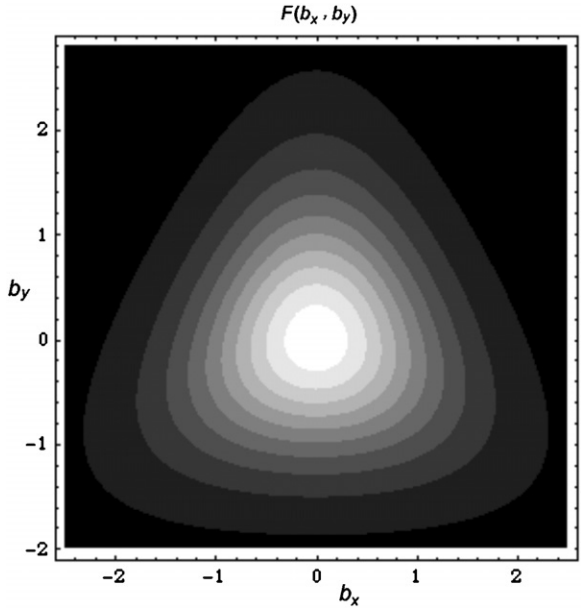

Figure 13. The contour plot of the 'Berry curvature' $F(b_x, b_y)$ from equation (97), as a function of control parameters b_x and b_y. Brighter areas correspond to larger values of $F(b_x, b_y)$ and the dark area corresponds to regions where $F(b_x, b_y) \approx 0$.

to this analogy, quantum-mechanical Berry phases appear to have counterparts in classical stochastic processes. The quantum pump effect, whose origin can be attributed to a Berry phase, has a stochastic counterpart with a similar geometric phase interpretation. We also showed that, as in quantum mechanics, geometric phases can influence the motion of coarse-grained degrees of freedom in stochastic processes after elimination of fast variables. This similarity raises questions about the possibility of further analogies.

Berry phases are responsible for a number of important effects in solid state physics, such as the quantum Hall effect. Although it is unclear whether or not similar effects can be discovered in classical dissipative systems, several features of the SPE have quantum-mechanical counterparts. We showed in section 10 that the SPE can be quantized, i.e. the number of system rotations per cycle can be some integer. Similar quantization has been considered as a special feature of the quantum pump [167] and the quantum Hall effect [19]. There are also examples of fractionally quantized responses of stochastic systems [133, 136]. Usually quantization is achieved in the limit of the maximum efficiency of the stochastic system response along a cycle in the space of control parameters. While such limits are easy to find in simple models, little is known about how to determine them in the general case. One possibility was proposed by Shi and Niu in [125]. Examining the diffusion in a periodic potential they related the quantization of the stochastic ratchet current to a Chern number. It is possible that this observation can be generalized within the Olson-Ao description of the Bloch–Peierls–Berry dynamics [169]. Another type of quantization was found in dissipative transport of a particle on a periodic lattice with non-Hermitian evolution [168].

Certainly, there are important differences between quantum and classical systems. The quantum Hall effect and the quantum theory of polarization require the existence of the Fermi sea, and thus are intrinsically many-body effects which rely on the Pauli principle for a multi-particle fermionic wavefunction. To some extent the Pauli principle can be mimicked

in stochastic processes by means of exclusion interactions, as in the theory of the shot noise in electronic circuits [103]. The model we discuss in section 5 provides a simple example of a geometric phase effect which is induced by exclusion interactions. Even in simple systems, interactions lead to important effects, such as violation of the assumptions of the no-pumping theorem [130, 136]. It is therefore important to explore geometric phases in strongly interacting many-body stochastic systems, such as in reaction-diffusion models and multistate exclusion processes [170, 171]. In quantum field theories, Berry phases are responsible for chiral anomalies [172]. Such anomalies play an important role in the quantum pump effect and in the theory of the quantum Hall effect [173]. It would be interesting to know whether the quantum-statistical analogies discussed in this review can be used to find stochastic phenomena analogous to chiral anomalies.

Conversely, quantum theory can benefit from the analogy with stochastic kinetics. For example, one can explore the possibility of a quantum-mechanical analogue of the pumping-restriction theorem. One can also consider geometric phases in the evolution of the counting statistics in quantum-mechanical systems [174]. Fractional quantization of pumping in stochastic systems, such as in [3]catenanes [133], may shed new light on the nature of quasiparticles in the fractional quantum Hall effect.

One of the goals of this review is to emphasize that geometric phases can play an important role in the theory of molecular motors. We showed that calculations of geometric phases are important in designing molecular motors and specifying their operations. Such calculations are not based on direct numerical solutions of differential equations with explicitly time-dependent parameters. Instead, by applying the theory of geometric phases it is possible to understand molecular motor operations using knowledge of only the energy landscape of a molecule as function of control parameters. The theory also suggests new response coefficients for experimental investigation. Measurements of the Berry curvature should provide new insight into the structure of motor molecules.

Molecular machines, driven by external time-dependent forces, obey simple universal laws, which remain to be explored and whose existence is indicated by the discovery of geometric phases in stochastic kinetics and exact universal results such as pumping-restriction theorems and fluctuation theorems. In the future, the science of controlled mesoscopic systems will be transformed by the investigation of these laws.

Acknowledgments

The author thanks Allan Adler for insightful comments, which were used to substantially improve this review. The author also thanks Qian Niu and Ilya Nemenman for useful discussions and Maryna Anatska for the help with illustrations. This work was funded in part by DOE under contract No. DE-AC52-06NA25396.

References

[1] Berry M V 1984 *Proc. R. Soc. Lond.* A **392** 45
[2] Chruscinski D and Jamiolkowski A 2004 *Geometric Phases in Classical and Quantum Mechanics* (Boston: Birkhäuser)
[3] Griffiths D J 2004 *Introduction to Quantum Mechanics* 2nd edn (New York: Benjamin-Cummings)
[4] Berry M 1990 *Phys. Today* **43** 34 (ISSN 0031-9228)
[5] Smit J 1955 *Physica* **21** 877
[6] Smit J 1958 *Physica* **24** 39
[7] Sinitsyn N A 2008 *J. Phys.: Condens. Matter* **20** 023201
[8] Murakami S, Nagaosa N and Zhang S-C 2003 *Science* **301** 1348

[9] Sinova J *et al* 2004 *Phys. Rev. Lett.* **92** 126603
[10] Resta R 2008 *J. Phys.: Conf. Ser.* **117** 012024
[11] Shalyt-Margolin A E, Strazhev V I and Tregubovich A Ya 2007 *Computer Science and Quantum Computing* (New York: Nova Science Publishers) p 125
[12] Lax M, Cai W and Xu M 2006 *Random Processes in Physics and Finance* (New York: Oxford University Press)
[13] Hannay J H 2006 *Am. J. Phys.* **74** 1
[14] Brockett R W 1976 *Proc. IEEE* **64** 61
[15] Murray R M, Li Z and Sastry S S 1994 *A Mathematical Introduction to Robotic Manipulation* (Boca Raton: CRC Press)
[16] Jarzynski C 1995 *Phys. Rev. Lett.* **74** 1732
[17] Kuvshinov V I and Kuzmin A V 2003 *Phys. Lett.* A **316** 391
[18] Whitney R S, Makhlin Y, Shnirman A and Gefen Y 2005 *Phys. Rev. Lett.* **94** 070407
[19] Zwanziger J *et al* 2003 *The Geometric Phase in Quantum Systems* (Berlin: Springer)
[20] Stehmann T, Heiss W D and Scholtz F G 2004 *J. Phys. A: Math. Gen.* **37** 7813
[21] Berry M V and Dennis M R 2003 *Proc. R. Soc. Lond.* A **459** 1261
[22] Shuvalov A L and Scott N H 2000 *Acta Mech.* **140** 1
[23] Garrison J C and Wright E M 1988 *Phys. Lett.* A **128** 177
[24] Dattoli G, Mignani R and Torre A 1990 *J. Phys. A: Math. Gen.* **23** 5795
[25] Berry M V 1990 *Proc. Math. Phys. Sci.* **430** 405
[26] Schilling R, Vogelsberger M and Garanin D A 2006 *J. Phys. A: Math. Gen.* **39** 13727
[27] Klyshko D N 1993 *Usp. Fiz. Nauk* **163** 1
[28] Jordan T F 1988 *J. Math. Phys.* **29** 2042
[29] Vinet L 1988 *Phys. Rev.* B **37** 2369
[30] Benedek C and Beenedict M G 1997 *Europhys. Lett.* **39** 347
[31] Han D, Kim Y S and Noz M E 1999 *Phys. Rev.* E **60** 1036
[32] Han D, Hardekopf E E and Kim Y S 1989 *Phys. Rev.* A **39** 1269
[33] Hannay J H 1985 *J. Phys. A: Math. Gen.* **18** 221
[34] Littlejohn R J 1988 *Phys. Rev.* A **38** 6034
[35] Ferraro R and Thibeault M 1999 *Eur. J. Phys.* **20** 143
[36] Mukunda N, Aravin P K and Simon R 2003 *J. Phys. A: Math. Gen.* **36** 2347
[37] Kitano M 1995 *Phys. Rev.* A **51** 4427
[38] Gerry Ch C 1989 *Phys. Rev.* A **39** 3204
[39] Kitano M and Yabuzaki T 1989 *Phys. Lett.* A **142** 321
[40] Sinitsyn N A and Saxena A 2008 *J. Phys. A: Math. Theor.* **41** 392002
[41] Choutri H, Maamache M and Menouar S 2002 *J. Korean Phys. Soc.* **40** 358
[42] Mehri-Dehnavi H and Mostafazadeh A 2008 *J. Math. Phys.* **49** 082105
[43] Mailybaev A A, Kirillov O N and Seyranian A P 2005 *Phys. Rev.* A **72** 014104
[44] Gunther U, Rotter I and Samsonov B F 2007 *J. Phys. A: Math. Theor.* **40** 8815
[45] Sun C P 1993 *Phys. Scr.* **48** 393
[46] Dembowski C *et al* 2004 *Phys. Rev.* E **69** 056216
[47] Dembowski C *et al* 2001 *Phys. Rev. Lett.* **86** 787
[48] Landsberg A S 1992 *Phys. Rev. Lett.* **69** 865
[49] Landsberg A S 1993 *Mod. Phys. Lett.* B **7** 71
[50] Ning C Z and Haken H 1991 *Phys. Rev.* A **43** 6410
[51] Ning C Z and Hanken H 1992 *Mod. Phys. Lett.* B **6** 1541
[52] Coullet P, Lega J and Pomeau Y 1991 *Eur. Phys. Lett.* **15** 221
[53] Sinitsyn N A, Dobrovitski V V, Urazhdin S and Saxena A 2008 *Phys. Rev.* B **77** 212405
[54] Frisch T, Rica S, Coullet P and Gilli J M 1994 *Phys. Rev. Lett.* **72** 1471
[55] Rudiger S, Casademunt J and Kramer L 2007 *Phys. Rev. Lett.* **99** 028302
[56] Kawagishi T, Mizuguchi T and Sano M 1995 *Phys. Rev. Lett.* **75** 3768
[57] Vierheilig A, Chevallard C and Gilli J M 1997 *Phys. Rev.* E **55** 7128
[58] Rudzick O and Mikhailov A S 2006 *Phys. Rev. Lett.* **96** 018302
[59] Scroggie A J, Gomila D, Firth W J and Oppo G L 2005 *Appl. Phys.* B **81** 963
[60] Abarzhi S I, Desjardins O, Nepomnyashchy A and Pitsch H 2007 *Phys. Rev.* E **75** 046208
[61] Maggipinto T, Brambilla M, Harkness G K and Firth W J 2000 *Phys. Rev.* E **62** 8726
[62] Toronov V Yu and Derbov V 1994 *Phys. Rev.* A **50** 878
[63] Toronov Yu and Derbov V L 1997 *Quantum Electron.* **27** 644
[64] Pomeau Y 1971 *Phys. Lett.* A **39** 143

[65] Pomeau Y 2002 *C. R. Phys.* **3** 1269
[66] Spivak B and Andreev V A 2009 *Phys. Rev. Lett.* **102** 063004
[67] Malozemoff A P and Slonczewski J C 1979 *Magnetic Domain Walls in Bubble Materials* (New York: Academic)
[68] Clarke D J *et al* 2008 arXiv:0806.2383
[69] Tretiakov O A, Clarke D, Chern G-W, Bazaliy Ya B and Tchernyshyov O 2008 *Phys. Rev. Lett.* **100** 127204
[70] Thiele A A 1973 *Phys. Rev. Lett.* **30** 230
[71] Shapere A and Wilczek F 1987 *Phys. Rev. Lett.* **58** 2051
Shapere A and Wilczek F 1988 *J. Fluid Mech.* **198** 557
[72] Shapere A and Wilczek F 1989 *Am. J. Phys.* **57** 514
[73] Purcell E M 1977 *Am. J. Phys.* **45** 3
[74] Childress S 1981 *Mechanics of Swimming and Flying* (Cambridge: Cambridge University Press)
[75] Lauga E and Powers T R 2008 arXiv:0812.2887
[76] Avron J E, Gat O and Kenneth O 2004 *Phys. Rev. Lett.* **93** 186001
[77] Najafi A and Golestanian R 2004 *Phys. Rev.* E **69** 062901
[78] Astumian R 2003 *AIP Conf. Proc.* **658** 221
[79] Avron J E, Kenneth O and Oaknin D H 2005 *New J. Phys.* **7** 234
[80] Golestanian R and Ajdari A 2008 *Phys. Rev. Lett.* **100** 038101
[81] Dreyfus R, Baudry J and Stone H A 2005 *Eur. Phys. J.* B **47** 161
[82] Dreyfus R *et al* 2005 *Nature Lett.* **437** 862
[83] Astumian R D and Dernyi I 2001 *Phys. Rev. Lett.* **86** 3859
[84] Westerhoff H V *et al* 1986 *Proc. Natl. Acad. Sci. USA* **83** 4734
[85] Robertson B and Astumian R D 1991 *J. Chem. Phys.* **94** 7414
[86] Robertson B and Astumian R D 1990 *Biophys. J.* **57** 689
[87] Astumian R D 2005 *J. Phys.: Condens. Matter* **17** S3753
[88] Buttiker M and Moskalets M 2006 *Lect. Notes Phys.* **690** 33
[89] Brouwer P W 1998 *Phys. Rev.* B **58** R10135
[90] Cohen D 2003 *Phys. Rev.* B **68** 155303
[91] Niu Q and Thouless D J 1984 *J. Phys. A: Math. Gen.* **17** 2453
[92] Vavilov M G 2005 *J. Phys. A: Math. Gen.* **38** 10587
[93] Mottonen M, Vartiainen J J and Pekola J P 2008 *Phys. Rev. Lett.* **100** 177201
[94] Geerligs L G, Anderegg V F, Holweg P A M and Mooij J E 1990 *Phys. Rev. Lett.* **64** 2691
[95] Blumental M D *et al* 2007 *Nature Phys.* **3** 343
[96] Tsong T Y and Chang C H 2003 *AAPPS Bull.* **13** 12
[97] Kallman E, Healy K and Siwy Z S 2007 *Europhys. Lett.* **78** 28002
[98] Astumian A D 2003 *Phys. Rev. Lett.* **91** 118102
[99] Ohkubo J 2008 *J. Stat. Mech.* P02011
[100] Sinitsyn N A and Nemenman I 2007 *Eur. Phys. Lett.* **77** 58001
[101] Sinitsyn N A and Nemenman I 2007 *Phys. Rev. Lett.* **99** 220408
[102] Ohkubo J 2008 *J. Chem. Phys.* **129** 205102
[103] Bagrets D A and Nazarov Y V 2003 *Phys. Rev.* B **67** 085316
[104] Michaelis L and Menten M L 1913 *Biochem. Z.* **49** 333
[105] Sukhorukov E V *et al* 2007 *Nature Phys.* **03** 243
[106] Jordan N and Sukhorukov E V 2004 *Phys. Rev. Lett.* **93** 260604
[107] Sukhorukov E V and Jordan A N 2007 *Phys. Rev. Lett.* **98** 136803
[108] Aharonov Y and Anandan J 1987 *Phys. Rev. Lett.* **58** 1593
[109] Pati A K 1998 *Ann. Phys.* **270** 178
[110] Sinitsyn N A and Nemenman I 2008 *Technical Report, LA-UR-08-04425*
[111] Elgart V and Kamenev A 2004 *Phys. Rev.* E **70** 051205
[112] Pilgram S *et al* 2003 *Phys. Rev. Lett.* **90** 206801
[113] Jordan A N, Sukhorukov E V and Pilgram S 2004 *J. Math. Phys.* **45** 4386
[114] Yarkony D R 1996 *Rev. Mod. Phys* **68** 985
[115] Sinitsyn N A 2007 *Phys. Rev.* B **76** 153314
[116] Elgart V and Kamenev A 2006 *Phys. Rev.* E **74** 041101
[117] Sinitsyn N A, Hengartner N and Nemenman I 2009 *Proc. Acad. Sci. USA* at press (arXiv:0808.4016)
[118] Ohkubo J 2007 *J. Stat. Mech.* P09017
[119] Kagan M L, Kepler T B and Epstein I R 1991 *Nature* **349** 506
Kepler T B and Kagan M L 1991 *Phys. Rev. Lett.* **66** 847

[120] Sinitsyn N A and Ohkubo J 2008 *J. Phys. A.: Math. Theor.* **41** 262002
[121] Gibbs J W 1873 *Trans. Conn. Acad.* **2** 309, 382
[122] Weinhold F 2009 *Classical and Geometrical Theory of Classical and Phase Thermodynamics* (Hoboken, NJ: Wiley)
[123] Markin S and Astumian R D 1990 *J. Chem. Phys.* **93** 5062
[124] Parrondo J M 1998 *Phys. Rev.* E **57** 7297
[125] Shi Y and Niu 2002 *Europhys. Lett.* **59** 324
[126] Mazenko G F 2006 *Nonequilibrium Statistical Mechanics* (New York: Wiley)
[127] Astumian R D 2009 *Phys. Rev.* E **79** 021119
[128] Lax M 1960 *Rev. Mod. Phys.* **32** 25
[129] Kenzaki H and Kikuchi M 2007 *Proteins: Struct. Funct. Bioinform.* **71** 389
[130] Rahav S, Horowitz J and Jarzynski C 2008 *Phys. Rev. Lett.* **101** 140602
[131] Chernyak V Y and Sinitsyn N A 2008 *Phys. Rev. Lett.* **101** 160601
[132] Baule A and Evans R M L 2008 *Phys. Rev. Lett.* **101** 240601
[133] Leigh D A *et al* 2003 *Nature* **424** 174
[134] Hernandez J V *et al* 2004 *Science* **306** 1532
[135] Sauvage J P 2001 *Molecular Mashines and Motors* (Berlin: Springer)
[136] Astumian D 2007 *Proc. Natl. Acad. Sci. USA* **104** 19715
[137] Jarzynski C 1998 *Acta Physica Polonica* B **29** 1609
[138] Andrieux D and Gaspard P 2007 *J. Stat. Phys.* **127** 107
[139] Astumian R D 2007 *Phys. Rev.* E **76** 020102
[140] Hill T L 1989 *Free Energy Transduction and Biochemical Cycle Kinetics* (New York: Dover)
[141] Harris R J and Schütz G M 2007 *J. Stat. Mech.: Theory Exp.* P07020
[142] Astumian R D and Chock P B 1989 *Phys. Rev.* A **39** 6416
[143] Astumian R D 2008 *Phys. Rev. Lett.* **101** 046802
[144] Kelly S D and Murray R M 1994 *CDS Technical Report 94-014* California Institute of Technology
[145] Bloch A, Crouch P, Baillieul J and Marsden J 2003 *Nonholonomic Mechanics and Control* (Berlin: Springer)
[146] Alberts B *et al* 2002 *Molecular Biology of the Cell* 4th edn (New York: Garland)
[147] Gelbart W M and Knobler C M 2008 *Phys. Today* 42
[148] Kay R E, Leigh D A and Zerbetto R 2007 *Angew. Chem. Int. Ed.* **46** 72
[149] Browne W R and Ferina B L 2006 *Nat. Nanotechnol.* **1** 25
[150] English B P *et al* 2006 *Nat. Chem. Biol.* **2** 87
[151] Kolomeisky A B and Fisher M E 2007 *Annu. Rev. Phys. Chem.* **58** 675
[152] Rostovtseva T K and Bezrukov M 1998 *Biophys. J.* **74** 2365
[153] Gopich I V and Szabo A 2006 *J. Chem. Phys.* **124** 154712
[154] Itoh H *et al* 2004 *Nature* **427** 465
[155] Soong R K *et al* 2001 *Biomed. Microdevices* **3** 71
[156] Kulic I M and Nelson P C 2008 *Europhys. Lett.* **81** 18001
[157] Tsong T Y and Chang C-H 2007 *BioSystems* **88** 323
[158] Hänggi P and Marchesoni F 2008 arXiv:0807.1283
[159] Reimann P 2002 *Phys. Rep.* **361** 57
[160] Jülicher F, Ajdari A and Prost J 1997 *Rev. Mod. Phys.* **69** 1269
[161] Astumian R D and Derenyl I 1998 *Eur. Biophys. J.* **27** 474
[162] Magnasco M O 1994 *Phys. Rev. Lett.* **72** 2656
[163] Qian H 2001 *Phys. Rev.* E **64** 022101
[164] Astumian A D and Hänggi P 2002 *Phys. Today* 33
[165] Hayashi K, Yamasaki H and Takano M 2009 arXiv:0901.0979
[166] de Ronde W H, Daniels B C, Mugler A, Sinitsyn N A and Nemenman I 2008 arXiv:0811.3283
[167] Flowers J L and Petley B W 2001 *Rep. Prog. Phys.* **64** 1191
[168] Rudner M S and Levitov L S 2009 *Phys. Rev. Lett.* **102** 065703
[169] Olson J C and Ao P 2007 *Phys. Rev.* B **75** 035114
[170] Chaudhuri A, Jain K, Marathe R and Dhar A 2007 *Phys. Rev. Lett.* **99** 190601
[171] Marathe R, Jain K and Dhar A 2008 *J. Stat. Mech.* P11014
[172] Bertlmann R A 2005 *Anomalies in Quantum Field Theories* (New York: Oxford University Press)
[173] Andreev A and Kamenev A 2000 *Phys. Rev. Lett.* **85** 1294
[174] Bel G, Zheng Y and Brown F L H 2006 *J. Chem. Phys.* B **110** 19066